

1 Site-level model intercomparison of high latitude and high 2 altitude soil thermal dynamics in tundra and barren landscapes

3
4 **A. Ekici¹, S. Chadburn², N. Chaudhary³, L. H. Hajdu⁴, A. Marmy⁵, S. Peng^{6,7}, J. Boike⁸,**
5 **E. Burke⁹, A. D. Friend⁴, C. Hauck⁵, G. Krinner⁶, M. Langer^{6,8}, P. A. Miller³, and C.**
6 **Beer¹⁰**

7
8 [1] {Department of Biogeochemical Integration, Max Planck Institute for Biogeochemistry, Jena,
9 Germany}

10 [2] {University of Exeter, Exeter, England}

11 [3] {Department of Physical Geography and Ecosystem Science, Lund University, Lund, Sweden}

12 [4] {Department of Geography, University of Cambridge, Cambridge, England}

13 [5] {Department of Geosciences, University of Fribourg, Fribourg, Switzerland}

14 [6] {Laboratoire de Glaciologie et Géophysique de l'Environnement, CNRS and Université
15 Grenoble Alpes, LGGE, F-38041, Grenoble, France}

16 [7] {Laboratoire des Sciences du Climat et de l'Environnement, France}

17 [8] {Alfred-Wegener-Institut, Helmholtz-Zentrum für Polar- und Meeresforschung, Potsdam,
18 Germany}

19 [9] {UK Met Office, England}

20 [10] {Department of Applied Environmental Science (ITM) and Bolin Centre for Climate Research,
21 Stockholm University, Stockholm, Sweden}

22 Correspondence to: A. Ekici (aekici@bgc-jena.mpg.de)

23 24 **Abstract**

25 Modelling soil thermal dynamics at high latitudes and altitudes requires representations of specific
26 physical processes such as snow insulation, soil freezing/thawing, as well as subsurface conditions
27 like soil water/ice content and soil texture type. We have compared six different land models
28 (JSBACH, ORCHIDEE, JULES, COUP, HYBRID8, LPJ-GUESS) at four different sites with
29 distinct cold region landscape types (i.e. Schilthorn-Alpine, Bayelva-high Arctic, Samoylov-wet
30 polygonal tundra, Nuuk-non permafrost Arctic) to identify the importance of physical processes in
31 capturing observed temperature dynamics in soils. This work shows how a range of models can
32 represent distinct soil temperature regimes in permafrost and non-permafrost soils. Snow insulation

1 is of major importance for estimating topsoil conditions, however soil physics is essential for the
2 subsoil temperature dynamics and thus the active layer thicknesses. Analyses show that land models
3 need more realistic surface processes (such as detailed snow dynamics and moss cover with
4 changing thickness/wetness) as well as better representations of subsoil thermal dynamics (i.e. soil
5 heat transfer mechanism and correct parameterization of heat conductivity/capacities).

6

7 **1 Introduction**

8 Recent atmospheric warming trends are affecting terrestrial systems by increasing soil temperatures
9 and causing changes in the hydrological cycle. Especially in high latitudes/altitudes, clear signs of
10 change are observed (Serreze et al., 2000; ACIA, 2005; IPCC AR5, 2013). These relatively colder
11 regions are characterized by the frozen state of terrestrial water, which makes soils more vulnerable
12 to warming by bringing the risk of shifting them into an unfrozen state. Such changes will have
13 broad implications for the physical (Romanovsky, 2010), biogeochemical (Schuur et al., 2008) and
14 structural (Larsen et al., 2008) conditions of the local, regional as well as global climate system.
15 Therefore, predicting the future state of the soil thermal regime at high latitudes and altitudes holds
16 major importance for Earth system modelling.

17 There are increasing concerns as to how land models perform at capturing high latitude soil thermal
18 dynamics, in particular in permafrost regions. Recent studies (Koven et al., 2013; Slater and
19 Lawrence, 2013) have provided detailed assessments of commonly used Earth System Models
20 (ESMs) in simulating soil temperatures of present and future state of the Arctic. By using the
21 Coupled Model Intercomparison Project phase 5 - CMIP5 (Taylor et al., 2009) results, Koven et al.
22 (2013) have shown a broad range of model outputs in estimating soil temperature. They attributed
23 most of the inter-model discrepancies to air-land surface coupling and snow representations in
24 models. Similar to those findings, Slater and Lawrence (2013) confirmed the high uncertainty of
25 CMIP5 models in predicting the permafrost state and their future trajectories. They have concluded
26 that the analyzed versions of models are not appropriate for such experiments since they lack
27 critical processes for cold region soils. Out of the many potential reasons, snow insulation, land
28 model physics, and vertical model resolutions were identified as being the major sources of
29 uncertainty.

30 Current land surface schemes and most of the vegetation and soil models represent energy and mass
31 exchange between the land surface and atmosphere in one dimension. Using a grid cell approach,
32 such exchanges are estimated for the entire land surface or specific regions. Therefore, comparing
33 simulated and observed time series of states or fluxes at point scale rather than grid averaging, is an
34 important component of model evaluation in order to understand remaining limitations of models
35 (Ekici et al., 2014; Mahecha et al., 2010). In such “site-level runs”, we assume that lateral processes

1 can be ignored and the ground thermal dynamics are mainly controlled by vertical processes. Then,
2 models are driven by observed climate and variables of interest can be compared to observations at
3 different temporal scales. Even though such idealized field conditions never exist, a careful
4 interpretation of site-level runs can identify major gaps in process representations in models.
5 In recent years, land models have improved their representations of the soil physical environment in
6 cold regions. Model enhancements include the addition of soil freezing/thawing, detailed snow
7 representations, prescribed moss cover, extending soil columns, and coupling soil heat transfer with
8 hydrology (Ekici et al., 2014; Gouttevin et al., 2012a; Dankers et al., 2011; Lawrence et al., 2008;
9 Wania et al., 2009a). Such improvements highlight the need for an updated assessment of model
10 performances in representing high latitude/altitude soil thermal dynamics.
11 We have compared the performances of six different land models in simulating soil thermal
12 dynamics at four contrasting sites. In comparison to previous works (Koven et al., 2013; Slater and
13 Lawrence, 2013), we used advanced model versions specifically improved for cold regions and our
14 model simulations are driven by (and evaluated with) site observations. To represent a wider range
15 of assessment and model structures, we used both land components of ESMs (JSBACH,
16 ORCHIDEE, JULES) and stand-alone models (COUP, HYBRID8, LPJ-GUESS), and compared
17 them at Arctic permafrost, Alpine permafrost and Arctic non-permafrost sites. By doing so, we
18 aimed to quantify the importance of different processes, to determine the general shortcomings of
19 current model versions and finally to highlight the key processes for future model developments.

20

21 **2 Methods**

22 **2.1 Model descriptions**

23 **2.1.1 JSBACH**

24 Jena Scheme for Biosphere-Atmosphere Coupling in Hamburg (JSBACH) is the land surface
25 component of the Max Planck Institute Earth System Model (MPI-ESM) that comprise ECHAM6
26 for the atmosphere (Stevens et al., 2012) and MPIOM for the ocean (Jungclauss et al., 2013). It
27 provides the land surface boundary for the atmosphere in coupled simulations; however, it can also
28 be used offline driven by atmospheric forcing. The current version of JSBACH (Ekici et al., 2014)
29 employs soil heat transfer coupled to hydrology with freezing and thawing processes included. The
30 soil model is discretized as five layers with increasing thicknesses up to 10 meters depth. There are
31 up to 5 snow layers with constant density and heat transfer parameters. JSBACH also simulates a
32 simple moss/organic matter insulation layer again with constant parameters.

33 **2.1.2 ORCHIDEE**

34 ORCHIDEE is a land surface model, which can be used coupled to the Institut Pierre Simon
35 Laplace (IPSL) climate model or driven offline by prescribed atmospheric forcing (Krinner et al.,

1 2005). ORCHIDEE computes all the soil-atmosphere-vegetation relevant energy and water
2 exchange processes in 30 min time steps. It combines a soil-vegetation-atmosphere transfer model
3 with a carbon cycle module computing vertically detailed soil carbon dynamics. The high latitude
4 version of ORCHIDEE includes a dynamic three-layer snow module (Wang et al., 2013), soil
5 freeze-thaw processes (Gouttevin et al., 2012a), and a vertical permafrost soil thermal and carbon
6 module (Koven et al., 2011). The soil hydrology is vertically discretized as 11 numerical nodes with
7 2m depth (Gouttevin et al., 2012a), and soil thermal and carbon modules are vertically discretized
8 as 32 layers with ~47m depth (Koven et al., 2011). One-dimensional Fourier equation was applied
9 to calculate soil thermal dynamics, and both soil thermal conductivity and heat capacity are
10 functions of the fraction of frozen and unfrozen soil water content and dry, saturated soil thermal
11 properties (Gouttevin et al., 2012b).

12 **2.1.3 JULES**

13 JULES (Joint UK Land Environment Simulator) is the land-surface scheme used in the Hadley
14 Centre climate model (Best et al., 2011; Clark et al., 2011), which can also be run offline, driven by
15 atmospheric forcing data. It is based on the Met Office Surface Exchange Scheme, MOSES (Cox et
16 al., 1999). JULES simulates surface exchange, vegetation dynamics and soil physical processes. It
17 can be run at a single point, or as a set of points representing a 2D grid. In each grid cell, the surface
18 is tiled into different surface types, and the soil is treated as a single column, discretized vertically
19 into layers (4 in the standard set-up). JULES simulates fluxes of moisture and energy between the
20 atmosphere, surface and soil, and the soil freezing and thawing. It includes a carbon cycle that can
21 simulate carbon exchange between the atmosphere, vegetation and soil. It also includes a multi-
22 layer snow model (Best et al., 2011), with layers that have variable thickness, density and thermal
23 properties. The snow scheme significantly improves the soil thermal regime in comparison with the
24 old, single-layer scheme (Burke et al., 2013). The model can be run with a timestep of between 30
25 minutes and 3 hours, depending on user preference.

26 **2.1.4 COUP**

27 COUP is a stand-alone, one-dimensional heat and mass transfer model for the soil-snow-
28 atmosphere system (Jansson and Karlberg, 2011) and is capable of simulating transient
29 hydrothermal processes in the subsurface including seasonal or perennial frozen ground (see e.g.
30 Hollesen et al. 2011; Scherler et al., 2010, 2013). Two coupled partial differential equations for
31 water and heat flow are the core of the COUP Model. They are calculated over up to 50 vertical
32 layers of arbitrary depth. Processes that are important for permafrost simulations, such as freezing
33 and thawing of the soil as well as the accumulation, metamorphosis, and melt of a snow cover are
34 included in the model (Lundin, 1990, Gustafsson et al., 2001). At temperatures above a threshold
35 temperature (-6 °C), unfrozen water coexists with ice. This approach respects the fact that in porous

1 media, liquid water coexists with frozen water at temperatures far below freezing point, due to high
2 pressure build up inside small pore spaces during freezing (Anderson et al., 1973). Freezing
3 processes in the soil are based on a function of freezing point depression and on an analogy of
4 freezing-thawing and wetting-drying (Harlan, 1973; Jansson and Karlberg, 2011). Snow cover is
5 simulated as one layer of variable height, density, and water content.

6 The upper boundary condition is given by a surface energy balance at the soil–snow–atmosphere
7 boundary layer, driven by air temperature, relative humidity, wind speed, global radiation, incoming
8 longwave radiation and precipitation. The lower boundary condition at the bottom of the soil
9 column is usually given by the geothermal heat flux (or zero heat flux) and a seepage flow of
10 percolating water. Water transfer in the soil depends on texture, porosity, water, and ice content.
11 Bypass flow through macropores, lateral runoff and rapid lateral drainage due to steep terrain can
12 also be considered (e.g. Scherler et al. 2013). A detailed description of the model including all its
13 equations and parameters is given in Jansson and Karlberg (2011) and Jansson (2012).

14 **2.1.5 HYBRID8**

15 HYBRID8 is a stand-alone land surface model, which computes the carbon and water cycling
16 within the biosphere and between the biosphere and atmosphere. It is driven by the daily/sub-daily
17 climate variables above the canopy, and the atmospheric CO₂ concentration. Computations are
18 performed on a 30-minute timestep for the energy fluxes, exchanges of carbon and water with the
19 atmosphere and the soil. Litter production and soil decomposition are calculated at a daily timestep.
20 HYBRID8 uses the surface physics and the latest parameterization of turbulent surface fluxes from
21 the GISS ModelE (Schmidt et al., 2006), but has no representation of vegetation dynamics. Also the
22 snow dynamics from modelE are not yet fully incorporated. Heat dynamics are described in
23 Rosenzweig et al. (1997) and moisture dynamics in Abramopoulos et al. (1998).

24 In HYBRID8 the prognostic variable for the heat transfer is the heat in the different soil layers and
25 from that the model evaluates the soil temperature. The processes governing this are the diffusion
26 from the surface to the different layers, as atmospheric forcing, and the conduction and advection
27 between the soil layers. The bottom boundary layer in HYBRID8 is impermeable resulting in zero
28 heat flux from below soil layers. The version used in this project has no representation of the snow
29 dynamics and has no insulating vegetation cover, however the canopy provides a simple heat buffer
30 due its separate heat capacity calculations.

31 **2.1.6 LPJ-GUESS**

32 Lund-Potsdam-Jena General Ecosystem Simulator (LPJ-GUESS) is a process-based model of
33 vegetation dynamics and biogeochemistry optimized for regional and global applications (Smith et
34 al., 2001). Mechanistic representations of biophysical and biogeochemical processes are shared
35 with those in the Lund-Potsdam-Jena dynamic global vegetation model LPJ-DGVM (Sitch et al.

1 2003; Gerten et al. 2004). However, LPJ-GUESS replaces the large area parameterization scheme
2 in LPJ-DGVM, whereby vegetation is averaged out over a larger area allowing several state
3 variables to be calculated in a simpler and faster manner, with more robust and mechanistic
4 schemes of individual- and patch-based resource competition and woody plant population
5 dynamics. Detailed descriptions are given by Smith et al. (2001), Sitch et al. (2003), Wolf et al.,
6 (2008), Miller and Smith (2012), and Zhang et al. (2013).

7 LPJ-GUESS has recently been updated to simulate Arctic upland and peatland ecosystems
8 (McGuire et al., 2012; Zhang et al., 2013). It shares the numerical soil thawing-freezing processes,
9 peatland hydrology and the model of wetland methane emission with LPJ-DGVM WHyMe, as
10 described by Wania et al. (2009a, 2009b, 2010). To simulate soil temperatures and active layer
11 depths, the soil column in LPJ-GUESS is divided into a single snow layer of fixed density and
12 variable thickness, a litter layer of fixed thickness (10 cm for these simulations, except for
13 Schilthorn where it is set to 2.5 cm), a soil column of 2 m depth (with sublayers of thickness 0.1 m,
14 each with a prescribed fraction of mineral and organic material, but with fractions of soil water and
15 air that are updated daily), and finally a “padding” column of depth 48 m (with thicker sublayers),
16 to simulate soil thermal dynamics. Insulation effects of snow, phase changes in soil water, daily
17 precipitation input and air temperature forcing are important determinants of daily soil temperature
18 dynamics at different sub-layers.

19 **2.2 Study sites**

20 **2.2.1 Nuuk**

21 The Nuuk observational site is located at southwestern Greenland. The site is situated in the
22 Kobbefjord at 500 m altitude above sea level and ambient conditions show arctic/polar climate
23 properties with a mean annual temperature of -1.5 °C in 2008 and -1.3 °C in 2009 (Jensen and
24 Rasch, 2009, 2010). Vegetation types consist of *Empetrum nigrum* with *Betula nana* and *Ledum*
25 *groenlandicum* with a vegetation height of 3-5 cm. The study site soil lacks mineral soil horizons
26 due to cryoturbation and lack of podsol development as it is placed on a dry location. Soil is
27 composed of 43% sand, 34% loam, 13% clay and 10% organic materials. No soil ice or permafrost
28 formations have been observed within the drainage basin. Snow cover is measured at the Climate
29 Basic station 1.65 km from the soil station but at the same altitude. At the time of the annual Nuuk
30 Basic snow survey in mid-April, the snow depth at the soil station was very similar to the snow
31 depth at the Climate Basic station: +/- 0.1 meter when the snow depth is high (near 1 meter). Strong
32 winds (>20 m/s) have a strong influence on the redistribution of newly fallen snow especially in the
33 beginning of the snow season, so the formation of a permanent snow cover at the soil station can be
34 delayed as much as one week, while the end of the snow cover season is similar to that at the
35 Climate Basic station (Birger Ulf Hansen, personal communication, 2013).

1 **2.2.2 Schilthorn**

2 The Schilthorn massif (Bernese Alps, Switzerland) is situated at 2970m altitude in the north central
3 part of the European Alps, and its non-vegetated lithology is dominated by deeply weathered
4 limestone schists forming a surface layer of mainly sandy and gravelly debris up to 5m thick over
5 presumably strongly jointed bedrock. Following the first indications of permafrost (ice lenses)
6 during the construction of the summit station between 1965 and 1967, the site was chosen for long-
7 term permafrost observation within the framework of the European PACE project and consequently
8 integrated into the Swiss permafrost monitoring network PERMOS as one of its reference sites
9 (PERMOS, 2013).

10 The measurements at the monitoring station at 2900m altitude are located on a flat plateau on the
11 north-facing slope and comprise a meteorological station and three boreholes (14m vertical, 100m
12 vertical and 100m inclined) with continuous ground temperature measurements since 1999 (Vonder
13 Mühl et al., 2000; Hoelzle and Gruber, 2008; Harris et al., 2009). Borehole data indicate
14 permafrost of at least 100m thickness, which is characterized by ice-poor conditions close to the
15 melting point. Maximum active-layer depths recorded since the start of measurements in 1999 are
16 generally around 4-6m, but during the exceptionally warm summer of the year 2003 the active-layer
17 depth increased to 8.6 m, reflecting the potential for degradation of permafrost at this site (Hilbich
18 et al., 2008).

19 The monitoring station is complemented by soil moisture measurements since 2007 and
20 geophysical (mainly geoelectrical) monitoring since 1999 (Hauck 2002, Hilbich et al. 2011). The
21 snow cover at the Schilthorn can reach maximum depths of about 2-3m and usually lasts from
22 October through to June/July. One dimensional soil model sensitivity studies showed that impacts
23 of long-term atmospheric changes would be strongest in summer and autumn, due to this late
24 snowmelt and the long decoupling of the atmosphere from the surface. So, increasing air
25 temperatures could lead to a severe increase in active-layer thickness (Engelhardt et al. 2010,
26 Marmy et al. 2013, Scherler et al. 2013).

27 **2.2.3 Samoylov**

28 Samoylov Island belongs to an alluvial river terrace of the Lena River Delta. The island is elevated
29 about 20 m above the normal river water level and covers an area of about 3.4 km² (Boike et al.
30 2013). The western part of the island constitutes a modern floodplain which is lowered compared to
31 the rest of the island and is often flooded during ice break-up of the Lena River in spring. The
32 eastern part of the island belongs to the elevated river terrace, which is mainly characterized by
33 moss, and sedge vegetated tundra (Kutzbach et al. 2007). In addition, several lakes and ponds occur
34 which make up about 25% of the surface area of Samoylov (Muster et al. 2012). The land surface of
35 the island is characterized by the typical micro-relief of polygonal patterned ground caused by frost

1 cracking and subsequent ice-wedge formation. The polygonal structures usually consist of
2 depressed centers, which are surrounded by elevated rims. The polygonal structures often occur in
3 different stages of degradation with partly to completely collapsed rims (Kutzbach et al. 2007). The
4 soil in the polygonal centers usually consists of water saturated sandy peat with the water table
5 standing a few centimeters below or above the surface. The elevated rims are usually covered with a
6 dry moss layer underlain by wet sandy soils with massive ice wedges underneath. The cryogenic
7 soil complex of the river terrace reaches depths of 10 to 15 m and is underlain by sandy to silty
8 river deposits. The deposits of the Lena River reach depths of at least 1 km in the delta region
9 (Langer et al. 2013).

10 There are strong spatial differences in surface energy balance due to highly fractionated surface and
11 subsurface properties. Due to thermo-erosion, there is an expansion of thermokarst lakes and small
12 ponds (Abnizova et al. 2012). Soil water drainage is strongly related to active layer dynamics,
13 lateral water flow occurs from late summer to autumn (Helbig et al. 2012). Site conditions include
14 strong snow-micro-topography, snow-vegetation interactions due to wind drift (Boike et al. 2013).

15 **2.2.4 Bayelva**

16 The Bayelva climate and soil-monitoring site is located in the Kongsfjord region at the west coast
17 of the Svalbard Island. The North Atlantic Current warms this area to an average air temperature of
18 about $-13\text{ }^{\circ}\text{C}$ in January and $+5\text{ }^{\circ}\text{C}$ in July, and provides about 400 mm precipitation annually,
19 falling mostly as snow between September and May. The annual mean temperature of 1994 to 2010
20 in Ny-Ålesund has been increasing by $+1.3\text{ K}$ per decade (Maturilli et al., 2013). The observation
21 site is located in the Bayelva River catchment on the Brøgger peninsula, about 3 km from the
22 village of Ny-Ålesund. The Bayelva catchment is bordered by two mountains, the Zeppelinfjellet
23 and the Scheteligfjellet, between which the glacial Bayelva River originates from the two branches
24 of the Brøggerbreen glacier moraine rubble. To the north of the study site, the terrain is flattening
25 and at about 1 km distance the Bayelva River reaches the shoreline of the Kongsfjorden (Arctic
26 Ocean). In the catchment area, sparse vegetation alternates with exposed soil and sand and rock
27 fields. Typical permafrost features, such as mud boils and non-sorted circles, are found in many
28 parts of the study area. The Bayelva permafrost site itself is located at 25 m a.s.l., on top of the
29 small Leirhaugen hill. The dominant ground pattern at the study site consists of non-sorted soil
30 circles. The bare soil circle centers are about 1 m in diameter and are surrounded by a vegetated rim
31 consisting of a mixture of low vascular plants of different species of grass and sedges (*Carex spec.*,
32 *Deschampsia spec.*, *Eriophorum spec.*, *Festuca spec.*, *Luzula spec.*), catchfly, saxifrage, willow and
33 some other local common species (*Dryas octopetala*, *Oxyria digyna*, *Polygonum viviparum*) and
34 unclassified species of mosses and lichens. The vegetation cover at the measurement site was
35 estimated to be approximately 60%, with the remainder being bare soil with a small proportion of

1 stones. The silty clay soil has a high mineral content, while the organic content is low, with organic
2 fractions below 10% (Boike et al., 2007). In the study period, the permafrost at Leirhaugen hill had
3 a mean annual temperature of about -2 °C at the top of the permafrost at 1.5 m depth.

4 Over the past decade, the Bayelva catchment has been the focus of intensive investigations into soil
5 and permafrost conditions (Roth and Boike, 2001; Boike et al., 2007; Westermann et al., 2010;
6 Westermann et al., 2011), the winter surface energy balance (Boike et al., 2003), and the annual
7 balance of energy, H₂O and CO₂, and micrometeorological processes controlling these fluxes
8 (Westermann et al. 2009; Lüers et al., 2014).

9 **2.3 Intercomparison set-up and simulation protocol**

10 In order to compare solely model representations of physical processes and eliminate any other
11 source of uncertainty (e.g. climate forcing, spatial resolution, soil parameters etc.), model
12 simulations are standardized as much as possible. Driving data for all site simulations were
13 prepared and distributed uniformly. Site observations were converted into continuous time series
14 with minor gap filling. Where the observed variable set lacked the variable needed by the models,
15 extended WATCH reanalysis data (Weedon et al., 2010; Beer et al., 2014) was used to complement
16 the data sets. Soil thermal properties are based on the sand, silt, and clay fractions of the
17 Harmonized World Soil database v1.1 (FAO et al., 2009). All model simulations are forced with
18 these datasets and the outputs from these site-level offline simulations are analyzed in this paper.
19 Table 3 summarizes the details of site driving data preparation together with soil static parameters.
20 To bring the state variables into equilibrium with climate, models are spun up with climate forcing
21 and the details are given in Table 4.

22 Most of the comparisons are performed for the upper part of the soil. The term “topsoil” is referred
23 from now on to indicate the chosen upper soil layer in each model and the first depth of soil
24 temperature observations. The details of layer selection are given in Table A1 of Appendix-A.

26 **3 Results and Discussions**

27 **3.1 Topsoil temperature and insulation effects**

28 Validation of topsoil temperature from observations and models gives an important estimate of the
29 accuracy of several model processes such as atmosphere-soil coupling, surface insulation, subsoil
30 thermal dynamics and hydrology. As all our study sites are located in cold climate zones (Fig. 1),
31 there is significant seasonality, which requires analyzing each season separately and inspecting key
32 seasonal processes. Figure 2 shows average seasonal topsoil temperature (see Table A1 for layer
33 depths) distributions extracted from the six models as well as the observed values at the four
34 different sites. In this figure, simulated temperatures show a wide range of values depending on
35 site-specific conditions and model formulations. Winter and spring comparisons have larger biases

1 than summer and autumn (Fig. 2). Observed winter and spring temperatures are much colder at
2 Samoylov than the other sites. Also there is a bigger range of temperature distribution at this site.
3 Observed summer temperatures are similar at all sites, although the non-permafrost Nuuk site has
4 warmer conditions than the others. For the modeled values, there is higher inconsistency in
5 capturing observed winter temperatures, especially at Samoylov and Schilthorn. Additionally the
6 modeled temperature range increases in spring. Even though the mean modeled temperatures are
7 closer to observed means in summer, the max and min values show a wide range of values during
8 this season. Autumn, however, shows a more uniform distribution of temperatures compared to
9 other seasons.

10 A proper assessment of critical processes entails examining seasonal changes in surface cover and
11 its consequent insulation effects for the topsoil temperature. As has been shown in a number of
12 studies (e.g. Koven et al., 2013; Scherler et al., 2013; Gubler et al., 2013; Fiddes et al., 2013)
13 modeled mean soil temperatures are strongly related to the atmosphere-surface thermal connection,
14 which is strongly influenced by snow cover and its properties. Snow cover can increase the mean
15 annual ground temperature and reduce the seasonal freezing depth (Zhang T., 2005). Figure 3
16 shows the seasonal relations between air and topsoil temperature at each study site. In this figure,
17 soil temperature values vary for each model with the same air temperature value, as all models are
18 driven with the same atmospheric forcing. When snow insulation protects the topsoil from cooling,
19 values lay above the 1:1 line. During the snow free season, when only vegetation cover, litter layers
20 or organic layer insulation protects the topsoil from warming, values stay below the 1:1 line.
21 However, insulation strength can change dramatically with critical levels of snow depth or dryness
22 of the vegetation cover. Aside from the insulation effects, the relation between air and topsoil
23 temperature depends also on atmosphere/topsoil temperature gradient, soil type/wetness and subsoil
24 temperatures.

25 The site observations show warmer topsoil temperatures than air during autumn, winter and spring
26 (Fig. 3). This situation indicates that soil is insulated when compared to colder air temperatures.
27 This can be attributed to the snow cover during these seasons (Fig. 4). High insulating property of
28 snow keeps the soil warmer than air, while not having snow usually results in colder topsoil
29 temperatures than air (as for the HYBRID8 model, cf. Fig. 3). Even though the high albedo of snow
30 provides a cooling effect for soil, the warming due to insulation dominates during most of the year.
31 Depending on their snow depth bias, models show different relations between air and topsoil
32 temperature. Figure 4 shows the changes in snow depth from observed and modeled values.
33 Compared to observations, the models that underestimate the snow depth at Nuuk and Bayelva (Fig.
34 4a, 4d) show colder topsoil temperature values in winter and are closer to the 1:1 line in Figure 3.
35 On the other hand, the amount of winter warm bias from snow depth overestimation in models

1 depends on whether the site has a “sub- or supra-critical” snow height. With supra-critical
2 conditions (e.g. at Schilthorn), the snow depth is so high that a small over/underestimation of the
3 model does not make a difference regarding the insulation. Only the timing of the snow arrival and
4 melt-out is important. In sub-critical conditions (e.g. at Samoylov), the snow depth is so low that
5 every overestimation leads automatically to a strong warm bias in the simulation e.g. for
6 JULES/COUP. This effect is also mentioned in Zhang T. (2005), where it is stated that snow depths
7 of less than 50 cm has the greatest impact on soil temperatures. However, overestimated snow depth
8 at Samoylov and Schilthorn does not always result in warmer soil temperatures in models as
9 expected (Fig. 3b, 3c). At these sites, even though JSBACH, JULES and COUP show warmer soil
10 temperatures in parallel to their snow depth overestimations, ORCHIDEE and LPJ-GUESS show
11 the opposite. This behavior indicates different processes working in opposite ways.

12 Nevertheless, most of winter, autumn and spring topsoil temperature biases can be explained by
13 snow conditions. For our study sites, the amount of snow depth bias is correlated with the amount
14 of topsoil temperature bias (Fig. 5). With overestimated (underestimated) snow depth, models
15 generally simulate warmer (colder) topsoil temperatures. As seen in Figure 5a, almost all models
16 underestimate the snow depth at Nuuk and Bayelva, and this created colder topsoil temperatures.
17 However, the overestimation of snow depth usually leads to warmer topsoil temperatures, but other
18 processes can compensate the warming and create a colder topsoil temperature (ORCHIDEE and
19 LPJ-GUESS values in Fig. 5 Samoylov and Schilthorn sites). Figure 5b shows that snow depth bias
20 can explain the topsoil temperature bias even when the snow free season is considered, which is due
21 to the long snow period at these sites (Table 2). This confirms the importance of snow
22 representation in models for capturing topsoil temperatures at high latitudes and high altitudes.

23 However, considering dynamic heat transfer parameters (volumetric heat capacity and heat
24 conductivity) in snow representation seems to be of lesser importance (JSBACH vs. other models,
25 see Table 1). This is related to the fact that most global models generally lack other important site-
26 specific snow processes such as strong wind drifts (creating patchy snow cover), depth hoar
27 formation and snow metamorphism (changing snow pack properties), snowmelt water infiltration
28 into soil (additional heat transfer mechanism) and snow albedo changes with these processes. As an
29 example, the landscape heterogeneity at Samoylov forms different soil thermal profiles for polygon
30 center and rim. While the soil temperature comparisons were performed for the polygon rim, snow
31 depth observations were taken from polygon center. Due to strong wind drift almost all snow is
32 removed from the rim and also limited to ca. 50cm (average polygon height) at the center (Boike et
33 al., 2008). This way, models are forced to overestimate snow depth and insulation, in particular on
34 the rim where soil temperature measurements have been taken. Hence, a resulting winter warm bias
35 is no surprise (Fig. 2a, models JSBACH, JULES, COUP).

1 During summer, observed values show warmer topsoil temperatures than air at Nuuk and Bayelva,
2 while the opposite is seen at Schilthorn and Samoylov (Fig. 3). Thicker moss cover and higher
3 moisture content at Samoylov (Boike et al., 2008) is the reason for better insulation (hence cooler
4 summer topsoil temperatures) at this site. Increasing thickness changes the heat storage of the moss
5 cover and acts as a stronger insulator (Gornall et al., 2007). Additionally, water content of the moss
6 layer affects the heat transfer parameters (Soudzilovskaia et al., 2013). However, without any plant
7 cover, the cooler topsoil temperatures at Schilthorn point to non-vegetation induced insulation in
8 summer. As snow can be persistent over spring season at high latitudes/altitudes and does not
9 completely disappear in summer months (Fig. 4), it is worthwhile to separate snow and snow free
10 seasons for these comparisons. Figure 6 shows the same atmosphere/topsoil temperature
11 comparison as in Figure 3 but using snow and snow free seasons instead of conventional seasons.
12 Evidently, without snow cover, the Schilthorn site indeed has warmer topsoil temperatures than air
13 as expected (Fig. 6b).

14 Insulation strength is lower during the snow-free season but the model results are inconsistent with
15 each other at all sites except Bayelva (Fig. 6). 10cm fixed moss cover in JSBACH and 10cm litter
16 layer in LPJ-GUESS brings similar amounts of insulation. At Samoylov, where strong vegetation
17 cover is observed in the field, these models perform better for snow free season (Fig. 6c). However,
18 at Bayelva, where vegetation effects are not that strong, 10cm insulating layer proves to be too
19 much and creates colder topsoil temperatures than observations (Fig. 6d). And for the bare
20 Schilthorn site, even a thin layer of surface cover (2.5 cm litter layer) creates colder topsoil
21 temperatures in LPJ-GUESS (Fig. 6b). At Bayelva, all models underestimate the observed topsoil
22 temperatures all year long (Fig. 6d). With underestimated snow depth (Fig. 4d) and winter cold bias
23 in topsoil temperature (Fig. 3d), models create a colder soil thermal profile that results in cooling of
24 the surface from below even during the snow free season. Furthermore, using global reanalysis
25 product instead of site observations (Table 3) might cause biases in incoming longwave radiation,
26 which can also affect the soil temperature calculations. In order to assess the model performance in
27 capturing observed soil temperature dynamics, it is important to drive the models with a complete
28 set of site observations.

29 These analyses support the need for such vegetation insulation in models during the snow free
30 season, but the spatial heterogeneity of surface vegetation thickness remains an important source of
31 uncertainty. More detailed moss representations were used in Porada et al. (2013) and Rinke et al.
32 (2008), and such approaches can improve the snow-free season insulation in models.

33 **3.2 Soil thermal regime**

34 Assessing soil thermal dynamics necessitates scrutinizing subsoil temperature dynamics as well as
35 surface conditions. Soil temperature evolutions of simulated soil layers are plotted for each model at

1 each site in Fig. 7-10. Although Nuuk is a non-permafrost site, most of the models simulate subzero
2 temperatures below 2-3 meters at this site (Fig. 7). At the same time, those models show colder
3 winter topsoil temperatures compared to observed values (Fig. 2a). Strong seasonal temperature
4 changes are observed close to the surface, whereas temperature amplitudes are reduced in deeper
5 layers and eventually a constant temperature is simulated at depths with zero annual amplitude
6 (DZAA). At Nuuk, only ORCHIDEE and COUP simulate a true DZAA at around 2.5-3 meters,
7 while all other models show a minor temperature change even at their deepest layers. Together with
8 the soil water/ice contents, simulating DZAA is partly related to the model soil depth and some
9 models are limited by their shallow depth representations (Table 1).

10 At the high altitude site Schilthorn (Fig. 8), JSBACH and JULES simulate above 0°C temperatures
11 (non-permafrost conditions) at deeper layers. In reality, there are almost isothermal conditions of
12 about -0.7°C between 7m and at least 100m depth at this site (PERMOS, 2013). This means a small
13 temperature mismatch (on the order of 1°C) can result in non-permafrost conditions. This kind of
14 temperature bias would not affect the permafrost condition at colder sites (e.g. Samoylov). In
15 addition, having low water and ice content, and a comparatively low albedo make the Schilthorn
16 site very sensitive to interannual variations and make it more difficult for models to capture the soil
17 thermal dynamics (Scherler et al., 2013). Compared to other models (with snow representation),
18 ORCHIDEE and LPJ-GUESS show colder subsurface temperatures at this site (Fig. 8), hence
19 hindering heat penetration from the surface. A thin surface litter layer (2.5cm) in LPJ-GUESS
20 contributes to the cooler Schilthorn soil temperatures in summer.

21 The simulated soil thermal regime at Samoylov reflects the colder climate at this site. All models
22 show subzero temperatures below 1m (Fig. 9). However, compared to other models, JULES and
23 COUP show values much closer to 0°C. As previously mentioned, subcritical snow conditions at
24 this site amplify the soil temperature overestimation coming from snow depth bias (Fig. 5).
25 Considering their better match during snow free season (Fig. 6c), the warmer temperatures in
26 deeper layers of JULES and COUP can be attributed to snow conditions at this site. Additionally,
27 these models include heat transfer via advection and conduction, while other models include just the
28 latter. Together, these effects create warmer soil profiles.

29 At the high-Arctic Bayelva site, all models create permafrost conditions (Fig. 10). The JULES and
30 COUP models again show warmer temperature profiles than the other models. These models
31 include soil heat transfer by advection that is lacked by other models. In combination with that,
32 COUP has a greater snow depth (Fig. 5), resulting in even warmer conditions than JULES. Such
33 conditions demonstrate the importance of the combined effects of surface processes together with
34 internal soil physics.

1 In general, permafrost specific model experiments require deeper soil representation than 5-10
2 meters. As discussed in Alexeev et al. (2007), at least 30 m soil depth is needed for capturing
3 decadal temperature variations in permafrost soils. The improvements from having such extended
4 soil depth are shown in Lawrence et al. (2012) when compared to their older model version with
5 shallow soil depth (Lawrence and Slater, 2005). Additionally, soil layer discretization plays an
6 important role for the accuracy of heat/water transfer within the soil, and hence can effect the ALT
7 estimations. Most of the models in our intercomparison have less than 10 m depths, so they lack
8 some effects of deep soil factors. However, most of the models used in global climate simulations
9 have similar soil depth representations and the scope here is to compare models that are not directly
10 aimed to simulate permafrost but to show general guidelines for future model developments.

11 Apart from the permafrost conditions, the heat transfer rate also differs among models. Internal soil
12 processes can impede the heat transfer and result in delayed warming or cooling of the deeper
13 layers. JSBACH, ORCHIDEE, JULES and COUP show a more pronounced time lag of the
14 heat/cold penetration into the soil, while HYBRID8 and LPJ-GUESS show either a very small lag
15 or no lag at all (Figs. 7-10). This time lag is affected by the method of heat transfer, soil heat
16 transfer parameters (soil heat capacity/conductivity), the amount of simulated phase change, vertical
17 soil model resolution and internal model timestep. Given that all models use similar heat transfer
18 methods including phase change (Table 1) and similar soil parameters (Table 3), the reason for the
19 rapid warming/cooling at deeper layers of some models can be the lower amount of latent heat
20 used/gained for the phase change, vertical resolution or model timestep. Even though the mineral
21 (dry) heat transfer parameters are shared among models, they are modified afterwards due to the
22 coupling of hydrology and thermal schemes. This leads to changes in the model heat conductivities
23 depending on how much water/ice they simulate in that particular layer. Unfortunately, not all
24 models output soil water/ice contents in a layered structure similar to soil temperature. This makes
25 it difficult to assess the differences in modelled phase change and the consequent changes to soil
26 heat transfer parameters. A better quantification of heat transfer rates would require a comparison of
27 simulated water contents and soil heat conductivities among models, which is beyond the scope of
28 this paper.

29 The soil thermal regime can also be investigated by studying the vertical temperature profiles
30 regarding the annual means (Fig. 11), and minimum and maximum values (Fig. 12). In Fig. 11, the
31 distribution of mean values is similar to the analysis of topsoil conditions. JSBACH and JULES and
32 COUP overestimate the temperatures at Schilthorn and Samoylov, but almost all models
33 underestimate it at Bayelva. Figure 12 shows the temperature envelopes of observed and simulated
34 values at each site. The min. (max.) temperature curve represents the coldest (warmest) possible
35 conditions for the soil thermal regime at a certain depth. The model biases in matching these curves

1 are related to their topsoil temperature bias, soil heat transfer mechanism and bottom boundary
2 conditions. Models without snow representation (e.g. HYBRID8) cannot match the min. curve in
3 Fig. 11-12. However, snow depth bias (Fig. 5) cannot explain the min. curve mismatch for
4 ORCHIDEE, COUP and LPJ-GUESS at Schilthorn (Fig. 11b). Furthermore, soil heat transfer
5 methods or the bottom boundary conditions do not seem to play an important role for matching
6 these soil temperature curves.

7 **3.3 Active layer thickness**

8 As it is affected by the soil temperature profile, soil hydrology, surface insulation and atmospheric
9 conditions; active layer thickness (ALT) is an integral measure of the soil thermal regime in
10 permafrost soils. Figure 13 shows the yearly change of ALT for the three permafrost sites. All
11 models overestimate the ALT at Samoylov (Fig. 13b), but there is disagreement among models in
12 overestimating or underestimating the ALT at Schilthorn (Fig. 13a) and Bayelva (Fig. 13c).

13 Surface conditions (e.g. insulation) alone are not enough to explain the soil thermal regime, which
14 affects ALT in turn. For Schilthorn, LPJ-GUESS generally shows shallower ALT values than other
15 models; however it also shows the largest snow depth bias (Fig. 5). If snow depth bias alone could
16 explain the ALT difference, ORCHIDEE would have to show different values than HYBRID8,
17 which completely lacks any snow representation. In addition to surface processes, subsoil
18 temperatures and soil water and ice contents affect the ALT. At Schilthorn, COUP has high snow
19 depth bias but still shows a very good match with ALT.

20 Overestimating snow depth (Fig. 5) and lacking the moss insulation (Fig. 6c) seems to match with
21 deeper ALT values in Samoylov (Fig. 13b). However, HYBRID8 does not have snow
22 representation, yet it shows the deepest ALT values, which means snow insulation is not the reason
23 for deeper ALT values in this model. Apart from not having any vegetation insulation, soil heat
24 transfer is also much faster in HYBRID8 (see section 3.2), which allows deeper penetration of
25 summer warming into the soil column.

26 Surface conditions alone cannot describe the ALT bias in Bayelva either. LPJ-GUESS shows the
27 lowest snow depth (Fig. 5) together with deepest ALT (Fig. 13c), while JULES shows similar snow
28 depth bias but the shallowest ALT values. As seen from Fig. 10, at this site LPJ-GUESS allows
29 deeper heat penetration due to its higher heat transfer rate. So, apart from the snow conditions, a
30 model's heat transfer rate is critical for predicting the ALT.

31 These results clearly show the risks of estimating ALT by topsoil temperatures alone. Many
32 previous studies (Lunardini, 1981; Kudryatsevet al., 1974; Romanovsky and Osterkamp, 1997;
33 Shiklomanov and Nelson, 1999; Stendel et al., 2007, Anisimov et al., 1997) used simple
34 relationships connecting topsoil temperatures and ALT. By doing so, they missed the effects of soil
35 internal factors on ALT. A good review of widely used analytical approximations and differences

1 to numerical approaches is given by Riseborough et al. (2008). More recently, Koven et al. (2013)
2 and Slater and Lawrence (2013) have highlighted large model uncertainties in estimating
3 permafrost extent and ALT values with similar approaches relating topsoil temperatures and
4 permafrost conditions in ESMs. However, other processes like the heat transfer scheme in the
5 subsurface layers and resulting water and ice contents are also important with regard to their impact
6 on the soil temperature profile, and hence the ALT. The equilibrium models are not capable to
7 estimate ALT in long-term simulations. So, using transient models and considering internal soil
8 physical factors are critical to properly assess ALT within climate change context.

9

10 **4 Conclusions**

11 We have evaluated different land models' soil thermal dynamics against observations using a site-
12 level approach. The analysis of the simulated soil thermal regime clearly reveals the importance of
13 reliable surface insulation for topsoil temperature dynamics and of reliable soil heat transfer
14 formulations for subsoil temperature and permafrost conditions at cold regions. Our findings
15 include the following conclusions.

- 16 1. At high latitudes and altitudes, model snow depth bias explains most of the topsoil
17 temperature biases.
- 18 2. The sensitivity of soil temperature to snow insulation depends on site snow conditions (sub-
19 /supra-critical).
- 20 3. Snow depth underestimation in models always leads to a cold bias in topsoil temperature,
21 whereas snow depth overestimation does not always lead to a warm bias in topsoil
22 temperatures.
- 23 4. Surface vegetation cover and litter/organic layer insulation is important for topsoil
24 temperatures in the snow free season, therefore models need more detailed representation of
25 moss and top organic layers.
- 26 5. Model heat transfer rates differ due to coupled heat transfer and hydrological processes. This
27 leads to discrepancies in subsoil thermal dynamics.
- 28 6. Surface processes alone cannot explain the whole soil profile's thermal regime; subsoil
29 conditions and model formulations affect the soil thermal dynamics.
- 30 7. Active layer thickness is related to both surface conditions and the soil thermal regime. ALT
31 estimation by topsoil temperatures can bring large errors.

32 For permafrost and cold region related soil experiments, it is important for models to simulate the
33 soil temperatures accurately, because permafrost extent, active layer thickness and the permafrost
34 soil carbon processes are strongly related to soil temperatures. There is a major concern on how soil
35 thermal state of these areas affect the ecosystem functions and what are the mechanisms

1 (physical/biogeochemical) relating atmosphere, oceans and soils in cold regions. With the currently
 2 changing climate, the strengths of these couplings will be altered bringing more uncertainty for
 3 future projections.

4 In this paper, we have shown the current state of some land models in capturing surface/subsurface
 5 temperatures at different cold region landscapes. It is evident that there is much uncertainty
 6 especially for above surface processes as well as soil internal physics of model formulations. To
 7 achieve better confidence in future simulations, model developments should include better
 8 insulation processes (for snow: compaction, metamorphism, depth hoar, wind drift; for moss:
 9 dynamic thickness and wetness) and more detailed evaluation of their soil heat transfer rates with
 10 observed data (comparing simulated ice contents and soil heat conductivities).

11

12 **Appendix A: Model layering schemes and depths of soil temperature**

13 **observations**

14 Table A1: Selected depths of observed and modeled soil temperatures referred as “topsoil
 15 temperature” in Figures 1, 2, 4, 5 and 6.

	Nuuk	Schilthorn	Samoylov	Bayelva
OBSERVATION	5 cm	20 cm	6 cm	6 cm
JSBACH	3.25 cm	18.5 cm	3.25 cm	3.25 cm
ORCHIDEE	6.5 cm	18.5 cm	6.5 cm	6.5 cm
JULES	5 cm	22.5 cm	5 cm	5 cm
COUP	5.5 cm	20 cm	2.5 cm	5.5 cm
HYBRID8	3.5 cm	22 cm	3.5 cm	3.5 cm
LPJ-GUESS	5 cm	25 cm	5 cm	5 cm

16

17 Exact depths of each soil layer used in model formulations:

18 **JSBACH:** 0.065, 0.254, 0.913, 2.902, 5.7 m

19 **ORCHIDEE:** 0.04, 0.05, 0.06, 0.07, 0.08, 0.1, 0.11, 0.14, 0.16, 0.19, 0.22, 0.27, 0.31, 0.37, 0.43,
 20 0.52, 0.61, 0.72, 0.84, 1.00, 1.17, 1.39, 1.64, 1.93, 2.28, 2.69, 3.17, 3.75, 4.42, 5.22,
 21 6.16, 7.27 m

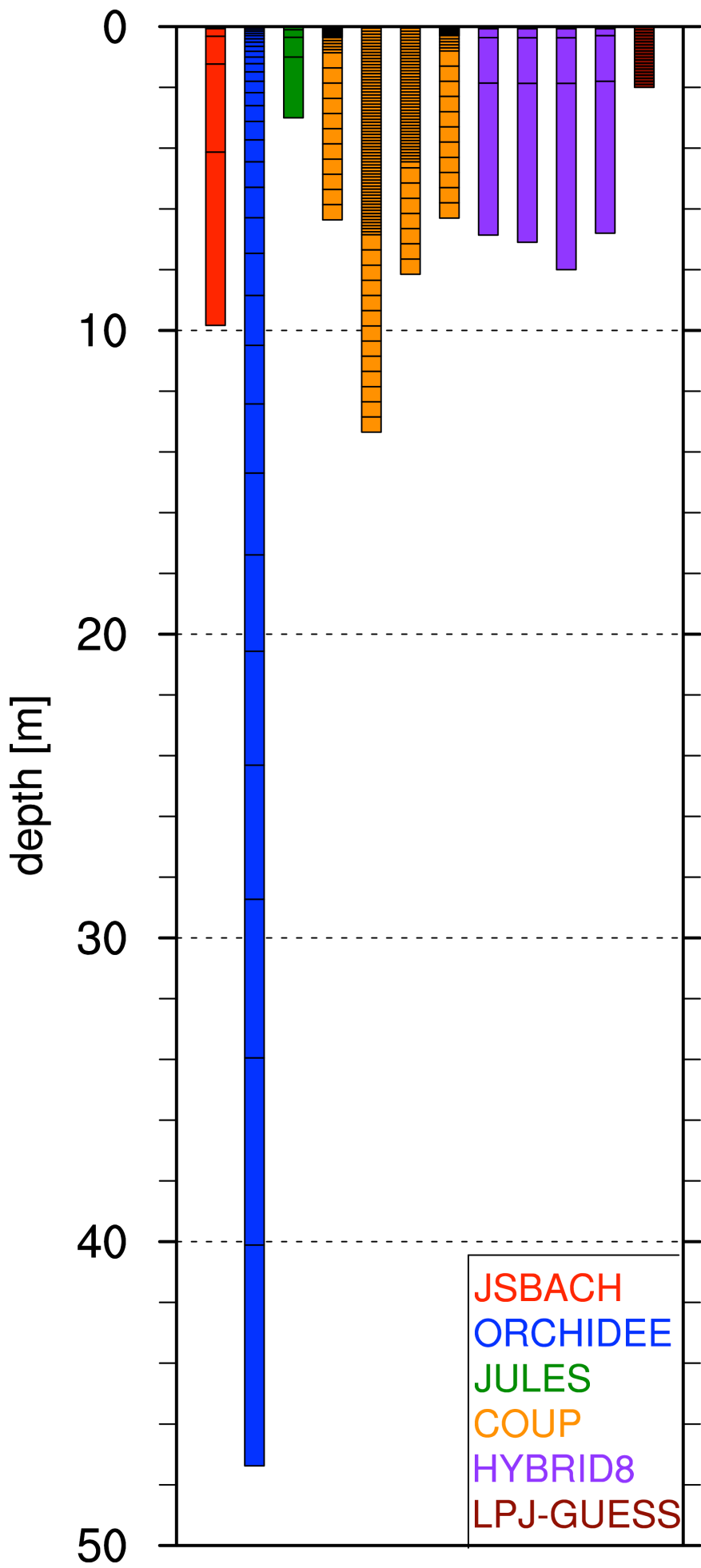
22 **JULES:** 0.1, 0.25, 0.65, 2.0 m

23 **COUP:** different for each site

24 Nuuk: 0.01 m intervals until 0.36 m, then 0.1 m intervals until 2 m and then 0.5 m intervals
 25 until 6 m

26 Schilthorn: 0.05 m then 0.1 m intervals until 7 m, and then 0.5 m intervals until 13 m

- 1 Samoylov: 0.05 m then 0.1 m intervals until 5 m, and then 0.5 m intervals until 8 m
- 2 Bayelva: 0.01 m intervals until 0.3 m, then 0.1 m intervals until 1 m and then 0.5 m intervals
- 3 until 6 m
- 4 **HYBRID8:** different for each site
- 5 Nuuk: 0.07, 0.29, 1.50, 5.00 m
- 6 Schilthorn: 0.07, 0.30, 1.50, 5.23 m
- 7 Samoylov: 0.07, 0.30, 1.50, 6.13 m
- 8 Bayelva: 0.07, 0.23, 1.50, 5.00 m
- 9 **LPJ-GUESS:** 0.1 m intervals until 2 m (additional padding layer of 48 m depth)
- 10
- 11 Depths of soil temperature observations for each site:
- 12 **NUUK:** 0.01,0.05,0.10,0.30 m
- 13 **SCHILTHORN:** 0.20,0.40,0.80,1.20,1.60,2.00,2.50,3.00,3.50,4.00,5.00,7.00,9.00,10.00 m
- 14 **SAMOYLOV:** 0.02,0.06,0.11,0.16,0.21,0.27,0.33,0.38,0.51,0.61,0.71 m
- 15 **BAYELVA:** 0.06,0.24,0.40,0.62,0.76,0.99,1.12 m



1 Figure A1: Soil layering schemes of each model. COUP and HYBRID8 models use different layering schemes for each
2 study site, which are represented with different bars (from left to right: Nuuk, Schilthorn, Samoylov and Bayelva).

4 **Acknowledgements**

5 The research leading to these results has received funding from the European Community's Seventh
6 Framework Programme (FP7 2007-2013) under grant agreement n° 238366. Authors also
7 acknowledge the BMBF project CarboPerm for the funding. Nuuk site monitoring data for this
8 paper were provided by the GeoBasis program run by Department of Geography, University of
9 Copenhagen and Department of Bioscience, Aarhus University, Denmark. The program is part of
10 the Greenland Environmental Monitoring (GEM) Program (www.g-e-m.dk) and financed by the
11 Danish Environmental Protection Agency, Danish Ministry of the Environment. We would like to
12 acknowledge a grant of the Swiss National Science Foundation (Sinergia TEMPS project, no.
13 CRSII2 136279) for the COUP model intercomparison, as well as the Swiss PERMOS network for
14 the Schilthorn data provided. Authors also acknowledge financial support from DEFROST, a Nordic
15 Centre of Excellence (NCoE) under the Nordic Top-level Research Initiative (TRI), and the Lund
16 University Centre for Studies of Carbon Cycle and Climate Interactions (LUCCI). Eleanor Burke
17 was supported by the Joint UK DECC/Defra Met Office Hadley Centre Climate Programme
18 (GA01101) and the European Union Seventh Framework Programme (FP7/2007-2013) under grant
19 agreement n°282700, which also provided the Samoylov site data.

21 **References**

- 22 Abnizova, A., Siemens, J., Langer, M., Boike, J.: Small ponds with major impact: The relevance of
23 ponds and lakes in permafrost landscapes to carbon dioxide emissions, *Global Biogeochemical*
24 *Cycles* 26 (2), 2012.
- 25 Abramopoulos, F., Rosenzweig, C., and Choudhury, B.: Improved ground hydrology calculations
26 for global climate models (GCMs): Soil water movement and evapotranspiration, *J. Climate*, 1,
27 921-941, doi:10.1175/1520-0442(1988)001<0921:IGHCFG>2.0.CO;2, 1988.
- 28 ACIA: Arctic Climate Impact Assessment, Cambridge University Press, New York, USA, 1042p,
29 2005.
- 30 Alexeev, V. A., Nicolsky, D. J., Romanovsky, V. E., and Lawrence, D. M.: An evaluation of deep
31 soil configurations in the CLM3 for improved representation of permafrost, *Geophys. Res.*
32 *Lett.*, 34, L09502, doi:10.1029/2007GL029536, 2007.
- 33 Anderson, D. M., Tice, A. R., and McKim, H. L.: The unfrozen water and the apparent specific heat
34 capacity of frozen soils, In *Permafrost: North American Contributions to the Second*

- 1 International Conference, Yakutsk, Siberia, USSR. National Academy of Sciences, Washington,
2 DC, 20418, 289–295, 1973.
- 3 Anisimov, O.A., and Nelson, F.E.: Permafrost zonation and climate change in the northern
4 hemisphere: results from transient general circulation models, *Climatic Change*, 35(2): 241–
5 258. DOI: 10.1023/A:1005315409698, 1997.
- 6 Beer, C., Weber, U., Tomelleri, E., Carvalhais, N., Mahecha, M., and Reichstein, M.: Harmonized
7 European long-term climate data for assessing the effect of changing temporal variability on
8 land-atmosphere CO₂ fluxes, *J. Climate*, 27, 4815–4834. doi: <http://dx.doi.org/10.1175/JCLI-D-13-00543.1>, 2014.
- 10 Best, M.J., Pryor, M., Clark, D.B., Rooney, G.G., Essery, R.L.H., Ménard, C.B., Edwards, J.M.,
11 Hendry, M.A., Porson, A., Gedney, N., Mercado, L.M., Sitch, S., Blyth, E., Boucher, O., Cox,
12 P.M., Grimmond, C.S.B., and Harding, R.J.: The Joint UK Land Environment Simulator
13 (JULES), model description – Part 1: Energy and water fluxes, *Geosci. Model Dev.*, 4, 677-699,
14 doi:10.5194/gmd-4-677-2011, 2011.
- 15 Boike, J., Roth, K., and Ippisch, O.: Seasonal snow cover on frozen ground: Energy balance
16 calculations of a permafrost site near Ny-Ålesund, Spitsbergen, *Journal of geophysical research-
17 atmospheres*, 108(D2)8163, 4, pp. 1-11, doi:10.1029/2001JD000939, 2003.
- 18 Boike, J., Ippisch, O., Overduin, P. P., Hagedorn, B., and Roth, K.: Water, heat and solute dynamics
19 of a mud boil, Spitsbergen, *Geomorphology*, 95 (1-2), 61-73,
20 doi:10.1016/j.geomorph.2006.07.033, 2007.
- 21 Boike, J., Wille, C., and Abnizova, A.: Climatology and summer energy and water balance of
22 polygonal tundra in the Lena River Delta, Siberia, *Journal of Geophysical Research*, Vol. 113,
23 G03025, doi: 10.1029/2007JG000540, 2008.
- 24 Boike, J., Kattenstroth, B., Abramova, K., Bornemann, N., Chetverova, A., Fedorova, I., Fröb, K.,
25 Grigoriev, M., Grüber, M., Kutzbach, L., Langer, M., Minke, M., Muster, S., Piel, K., Pfeiffer,
26 E.-M., Stoof, G., Westermann, S., Wischnewski, K., Wille, C., and Hubberten, H.-W.: Baseline
27 characteristics of climate, permafrost and land cover from a new permafrost observatory in the
28 Lena River Delta, Siberia (1998–2011), *Biogeosciences* 10 (3), 2105–2128, 2013.
- 29 Burke, E.J., Dankers, R., Jones, C.D., and Wiltshire, A.J.: A retrospective analysis of pan Arctic
30 permafrost using the JULES land surface model, *Climate Dynamics*, Volume 41, Issue 3-4, pp
31 1025-1038, 2013.
- 32 Clark, D.B., Mercado, L.M., Sitch, S., Jones, C.D., Gedney, N., Best, M.J., Pryor, M., Rooney
33 G.G., Essery, R.L.H., Blyth, E., Boucher, O., Harding, R.J., Huntingford, C., and Cox, P.M.:
34 The Joint UK Land Environment Simulator (JULES), model description – Part 2: Carbon fluxes
35 and vegetation dynamics, *Geosci. Model Dev.*, 4, 701-722, doi:10.5194/gmd-4-701-2011, 2011.

- 1 Cox, P.M., Betts, R.A., Bunton, C.B., Essery, R.L.H., Rowntree, P.R., and Smith, J.: The impact of
2 new land surface physics on the GCM simulation of climate and climate sensitivity, *Clim.*
3 *Dynam.*, 15:183–203, 1999.
- 4 Dankers, R., Burke, E. J., and Price, J.: Simulation of permafrost and seasonal thaw depth in the
5 JULES land surface scheme, *The Cryosphere*, 5(3), 773–790, 2011.
- 6 Ekici, A., Beer, C., Hagemann, S., Boike, J., Langer, M., and Hauck, C.: Simulating high-latitude
7 permafrost regions by the JSBACH terrestrial ecosystem model, *Geosci. Model Dev.*, 7, 631-
8 647, doi:10.5194/gmd-7-631-2014, 2014.
- 9 Engelhardt, M., Hauck, C., and Salzmann, N.: Influence of atmospheric forcing parameters on
10 modelled mountain permafrost evolution, *Meteorologische Zeitschrift*, 19(5), 491-500, 2010.
- 11 FAO, IIASA, ISRIC, ISS-CAS, and JRC: Harmonized World Soil Database (version 1.1) FAO,
12 Rome, Italy and IIASA, Laxenburg, Austria, 2009.
- 13 Fiddes, J., Endrizzi, S., and Gruber, S.: Large area land surface simulations in heterogeneous terrain
14 driven by global datasets: application to mountain permafrost, *The Cryosphere Discussions*,
15 7(6), 5853-5887, 2013.
- 16 Friend, A.D.: Terrestrial plant production and climate change: *Journal of Experimental Botany* 61,
17 1293-1309, doi:10.1093/jxb/erq019, 2010.
- 18 Friend, A.D., and Kiang, N.Y.: Land-surface model development for the GISS GCM: Effects of
19 improved canopy physiology on simulated climate, *Journal of Climate* 18, 2883-2902,
20 doi:10.1175/JCLI3425.1, 2005.
- 21 Friend, A.D., Geider, R.J., Behrenfeld, M.J., and Still, C.J.: Photosynthesis in Global-Scale Models,
22 In: *Photosynthesis in silico: Understanding Complexity from Molecules to Ecosystems*, Laisk
23 A, Nedbal L, Govindjee (Eds), Springer Series "Advances in Photosynthesis and Respiration".
24 Vol 29, Springer (Dordrecht, The Netherlands), pp. 465-497, 2009.
- 25 Gerten, D., Schaphoff, S., Haberlandt, U., Lucht, W., and Sitch, S.: Terrestrial vegetation and water
26 balance – hydrological evaluation of a dynamic global vegetation model, *Journal of Hydrology*
27 286: 249–270, 2004.
- 28 Gornall, J.L., Jonsdottir, I.S., Woodin, S.J., and Van der Wal, R.: Arctic mosses govern below-
29 ground environment and ecosystem processes, *Oecologia*, 153, 931–941, doi:10.1007/s00442-
30 007-0785-0, 2007.
- 31 Gouttevin, I., Krinner, G., Ciais, P., Polcher, J., and Legout, C.: Multi-scale validation of a new soil
32 freezing scheme for a land-surface model with physically-based hydrology, *The Cryosphere*, 6,
33 407-430, doi:10.5194/tc-6-407-2012, 2012a.

1 Gouttevin, I., M. Menegoz, F. Domine, G. Krinner, C. D. Koven, P. Ciais, C. Tarnocai, and J.
2 Boike: How the insulating properties of snow affect soil carbon distribution in the continental
3 pan-Arctic area, *J. Geophys. Res.*, doi:10.1029/2011JG001916, 2012b.

4 Gubler, S., Endrizzi, S., Gruber, S., and Purves, R. S.: Sensitivities and uncertainties of modeled
5 ground temperatures in mountain environments, *Geosci. Model Dev.*, 6, 1319–1336, 2013.

6 Gustafsson, D., Stähli, M., and Jansson, P.-E.: The surface energy balance of a snow cover:
7 comparing measurements to two different simulation models, *Theor. Appl. Climatol.*, 70, 81–
8 96, 2001.

9 Harlan, R. L.: Analysis of coupled heat-fluid transport in partially frozen soil, *Water Resour. Res.*,
10 9, 1314–1323, 1973.

11 Harris, C., Arenson, L., Christiansen, H., Etzelmüller, B., Frauenfelder, R., Gruber, S., Haeberli,
12 W., Hauck, C., Hoelzle, M., Humlum, O., Isaksen, K., Käab, A., Kern-Lütschg, M., Lehning,
13 M., Matsuoka, N., Murton, J., Nötzli, J., Phillips, M., Ross, N., Seppälä, M., Springman, S.,
14 Vonder Mühll, D.: Permafrost and climate in Europe: monitoring and modelling thermal,
15 geomorphological and geotechnical responses, *Earth Science Reviews* 92 (3-4), 117-171, 2009.

16 Hauck, C.: Frozen ground monitoring using DC resistivity tomography. *Geophysical Research*
17 *Letters*, 29 (21): 2016, doi: 10.1029/2002GL014995, 2002.

18 Helbig, M., Boike, J., Langer, M., Schreiber, P., Runkle, B.R., and Kutzbach, L.: Spatial and
19 seasonal variability of polygonal tundra water balance: Lena River Delta, northern Siberia
20 (Russia), *Hydrogeology Journal* 21 (1), 133–147, 2013.

21 Hilbich, C., Hauck, C., Hoelzle, M., Scherler, M., Schudel, L., Völksch, I., Vonder Mühll, D., and
22 Mäusbacher, R.: Monitoring mountain permafrost evolution using electrical resistivity
23 tomography: A 7-year study of seasonal, annual, and long-term variations at Schilthorn, Swiss
24 Alps, *J. Geophys. Res.*, 113, F01S90, doi:10.1029/2007JF000799, 2008.

25 Hilbich, C., Fuss, C., and Hauck, C.: Automated time-lapse ERT for improved process analysis and
26 monitoring of frozen ground, *Permafrost and Periglacial Processes* 22(4), 306-319, DOI:
27 10.1002/ppp.732, 2011.

28 Hoelzle, M., Gruber, S.: Borehole and ground surface temperatures and their relationship to
29 meteorological conditions in the Swiss Alps, In: Kane, D.L., Hinkel, K.M, (Eds.), *Proceedings*
30 *Ninth International Conference on Permafrost*, June 29–July 3, Fairbanks Alaska, vol. 1.
31 Institute of Northern Engineering, University of Alaska Fairbanks, pp. 723–728, 2008.

32 Hollesen, J., Elberling, B. and Jansson, P.E.: Future active layer dynamics and carbon dioxide
33 production from thawing permafrost layers in Northeast Greenland, *Global Change Biology*,
34 17: 911–926. doi: 10.1111/j.1365-2486.2010.02256.x, 2011.

1 IPCC AR5: Summary for Policymakers, Climate Change 2013, The Physical Science Basis,
2 Contribution of Working Group I to the Fifth Assessment Report of the Intergovernmental
3 Panel on Climate Change [Stocker, T.F., D. Qin, G.-K. Plattner, M. Tignor, S. K. Allen, J.
4 Boschung, A. Nauels, Y. Xia, V. Bex and P.M. Midgley (eds.)], Cambridge University Press,
5 Cambridge, United Kingdom and New York, NY, USA, 2013.

6 Jansson, P.E.: CoupModel: model use, calibration, and validation, Transactions of the ASABE 55.4,
7 1335-1344, 2012.

8 Jansson, P.-E. and Karlberg, L.: Coupled heat and mass transfer model for soil-plant-atmosphere
9 systems, Royal Institute of Technology, Dept of Civil and Environmental Engineering,
10 Stockholm, available at: <http://www.lwr.kth.se/Vara%20Datorprogram/CoupModel/index.htm>,
11 2011.

12 Jensen, L.M., and Rasch, M.: Nuuk Ecological Research Operations, 2nd Annual Report, 2008,
13 Roskilde, National Environmental Research Institute, Aarhus University, Denmark, 80 pp.,
14 2009.

15 Jensen, L.M., and Rasch, M.: Nuuk Ecological Research Operations, 3rd Annual Report, 2009,
16 Roskilde, National Environmental Research Institute, Aarhus University, Denmark, 80 pp.,
17 2010.

18 Jungclaus, J. H., Fischer, N., Haak, H., Lohmann, K., Marotzke, J., Matei, D., Mikolajewicz, U.,
19 Notz, D., and von Storch, J. S.: Characteristics of the ocean simulations in MPIOM, the ocean
20 component of the MPI-Earth System Model, *J. Adv. Model. Earth Syst.*, 5, 422–446,
21 doi:10.1002/jame.20023, 2013.

22 Koven, C.D., Ringeval, B., Friedlingstein, P., Ciais, P., Cadule, P., Khvorostyanov, D., Krinner, G.,
23 and Tarnocai, C.: Permafrost carbon-climate feedbacks accelerate global warming, *Proceedings*
24 *of the National Academy of Sciences*, 2011.

25 Koven, C.D., William, J.R., and Alex, S.: Analysis of Permafrost Thermal Dynamics and Response
26 to Climate Change in the CMIP5 Earth System Models. *J. Climate*, 26, 1877–1900. doi:
27 <http://dx.doi.org/10.1175/JCLI-D-12-00228.1>, 2013.

28 Krinner, G., Viovy, N., de Noblet-Ducoudré, N., Oge' e, J., Polcher, J., Friedlingstein, P., Ciais, P.,
29 Sitch, S., and Prentice, I.C.: A dynamic global vegetation model for studies of the coupled
30 atmosphere-biosphere system, *Global Biogeochem. Cycles*, 19, GB1015,
31 doi:10.1029/2003GB002199, 2005.

32 Kudryavtsev, V.A., Garagulya, L.S., Kondrat'yeva, K.A., and Melamed, V.G.: Fundamentals of
33 Frost Forecasting in Geological Engineering Investigations, Cold Regions Research and
34 Engineering Laboratory: Hanover, NH, 1974.

- 1 Kutzbach, L., Wille, C., and Pfeiffer, E.: The exchange of carbon dioxide between wet arctic tundra
2 and the atmosphere at the Lena River Delta, Northern Siberia, *Biogeosciences* 4, 869–890,
3 2007.
- 4 Langer, M., Westermann, S., Heikenfeld, M., Dorn, W., and Boike, J.: Satellite-based modeling of
5 permafrost temperatures in a tundra lowland landscape, *Remote Sensing of Environment*,
6 135, 12–24, doi:10.1016/j.rse.2013.03.011, 2013.
- 7 Larsen, P. H., Goldsmith, S., Smith, O., Wilson, M.L., Strzepek, K., Chinowsky, P., and Saylor, B.:
8 Estimating future costs for Alaska public infrastructure at risk from climate change, *Global*
9 *Environ. Change*, 18, 442–457, doi:10.1016/j.gloenvcha.2008.03.005, 2008.
- 10 Lawrence, D. M. and Slater, A. G.: A projection of severe near- surface permafrost degradation
11 during the 21st century, *Geophys. Res. Lett.*, 32, L24401, doi:10.1029/2005GL025080, 2005.
- 12 Lawrence, D. M., Slater, A. G., Romanovsky, V. E., and Nicolsky, D. J.: Sensitivity of a model
13 projection of near-surface permafrost degradation to soil column depth and representation of
14 soil organic matter, *J. Geophys. Res.*, 113, 1–14, 2008.
- 15 Lawrence, D. M., Slater, A. G., and Swenson, S. C.: Simulation of Present-Day and Future
16 Permafrost and Seasonally Frozen Ground Conditions in CCSM4, *J. C Climate*, 25, 2207–2225,
17 2012.
- 18 Lunardini, V.J.: Heat transfer in cold climates, Van Nostrand Reinhold: New York, 1981.
- 19 Lundin, L. C.: Hydraulic properties in an operational model of frozen soil, *J. Hydrol.*, 118, 289–
20 310, 1990.
- 21 Lüers, J., Westermann, S., Piel, K., and Boike, J.: Annual CO₂ budget and seasonal CO₂ exchange
22 signals at a High Arctic permafrost site on Spitsbergen, Svalbard archipelago, *Biogeosciences*
23 *Discuss.*, 11, 1535-1559, doi:10.5194/bgd-11-1535-2014, 2014.
- 24 Mahecha, M. D., Reichstein, M., Jung, M., Seneviratne, S.I., Zaehle, S., Beer, C., Braakhekke,
25 M.C., Carvalhais, N., Lange, H., Le Maire G., and Moors, E.: Comparing observations and
26 process-based simulations of biosphere-atmosphere exchanges on multiple timescales, *J.*
27 *Geophys. Res.*, 115, G02003, doi:10.1029/2009JG001016, 2010.
- 28 Marmy, A., Salzmann, N., Scherler, M., and Hauck, C.: Permafrost model sensitivity to seasonal
29 climatic changes and extreme events in mountainous regions, *Environmental Research Letters*,
30 8(3), 035048, 2013.
- 31 Maturilli, M., Herber, A., and König-Langlo, G.: Climatology and time series of surface
32 meteorology in Ny-Ålesund, Svalbard, *Earth Syst. Sci. Data*, 5, 155-163, doi:10.5194/essd-5-
33 155-2013, 2013.
- 34 McGuire, A. D., Christensen, T. R., Hayes, D., Heroult, A., Euskirchen, E., Kimball, J. S.,
35 Koven, C., Lafleur, P., Miller, P. A., Oechel, W., Peylin, P., Williams, M., and Yi, Y.: An

1 assessment of the carbon balance of Arctic tundra: comparisons among observations, process
2 models, and atmospheric inversions, *Biogeosciences*, 9, 3185-3204, doi:10.5194/bg-9-3185-
3 2012, 2012.

4 Miller, P.A., and Smith, B.: Modeling tundra vegetation response to recent Arctic warming,
5 *AMBIO, J. Human. Environ.*, 41, 281–291, 2012.

6 Muster, S., Langer, M., Heim, B., Westermann, S., and Boike, J.: Subpixel heterogeneity of ice-
7 wedge polygonal tundra: a multi-scale analysis of land cover and evapotranspiration in the Lena
8 River Delta, Siberia, *Tellus B*, 64, 2012.

9 PERMOS: Permafrost in Switzerland 2008/2009 and 2009/2010, Noetzli, J. (ed.), Glaciological
10 Report (Permafrost) No. 10/11 of the Cryospheric Commission of the Swiss Academy of
11 Sciences (SCNAT), Zurich, Switzerland, 2013.

12 Porada, P., Weber, B., Elbert, W., Pöschl, U., and Kleidon, A.: Estimating global carbon uptake by
13 Lichens and Bryophytes with a process-based model, *Biogeosciences*, 10 (6989-7033),
14 doi:10.5194/bg-10-6989-2013, 2013.

15 Rinke, A., Kuhry, P., and Dethloff, K.: Importance of a soil organic layer for Arctic climate: A
16 sensitivity study with an Arctic RCM, *Geophys. Res. Lett.*, 35, L13709,
17 doi:10.1029/2008GL034052., 2008.

18 Riseborough, D., Shiklomanov, N., Etzelmuller, B., Gruber, S., and Marchenko, S.: Recent
19 Advances in Permafrost Modelling, *Permafr. Periglac. Process.*, 19, 137–156, 2008.

20 Romanovsky, V.E., and Osterkamp, T.E.: Thawing of the active layer on the coastal plain of the
21 Alaskan Arctic, *Permafrost and Periglacial Processes*, 8(1): 1–22. DOI: 10.1002/(SICI)1099-
22 1530(199701)8:1<1::AID-PPP243 >3.0.CO;2-U, 1997.

23 Romanovsky, V.E., Smith, S.L., and Christiansen, H.H.: Permafrost thermal state in the polar
24 Northern Hemisphere during the international polar year 2007-2009: a synthesis, *Permafr.*
25 *Periglac. Process.*, 21, 106–116, 2010.

26 Rosenzweig, C. and Abramopoulos, F.: Land-surface model development for the GISS GCM, *J.*
27 *Climate*, 10, 2040-2054, doi:10.1175/1520-0442(1997)010<2040:LSMDFT>2.0.CO;2,1997.

28 Roth, K. and Boike, J.: Quantifying the thermal dynamics of a permafrost site near Ny-Ålesund,
29 Svalbard., *Water resources research*, 37 (12), pp. 2901-2914, doi: 10.1029/2000WR000163,
30 2001.

31 Schaefer, K., Zhang, T., Slater, A.G., Lu, L., Etringer, A. and Baker, I.: Improving simulated soil
32 temperatures and soil freeze/thaw at high-latitude regions in the Simple Biosphere/Carnegie-
33 Ames-Stanford Approach model, *J. Geophys. Res.*, 114, F02021, doi:10.1029/2008JF001125,
34 2009.

- 1 Scherler, M., Hauck, C., Hoelzle, M., Stähli, M. and Völksch, I.: Meltwater infiltration into the
2 frozen active layer at an alpine permafrost site, *Permafrost Periglac. Process.*, 21: 325–334,
3 doi: 10.1002/ppp.694, 2010.
- 4 Scherler, M., Hauck, C., Hoelzle, M., and Salzmann, N.: Modeled sensitivity of two alpine
5 permafrost sites to RCM-based climate scenarios, *J. Geophys. Res. Earth Surf.*, 118,
6 doi:10.1002/jgrf.20069, 2013.
- 7 Schmidt, G.A., Ruedy, R., Hansen, J.E., Aleinov, I., Bell, N., Bauer, M., Bauer, S., Cairns, B.,
8 Canuto, V., Cheng, Y., Del Genio, A., Faluvegi, G, Friend, A.D., Hall, T.M., Hu, Y., Kelley,
9 M., Kiang, N.Y., Koch, D., Lacis, A.A., Lerner, J., Lo, K.K., Miller, R.L., Nazarenko, L.,
10 Oinas, V., Perlwitz, Ja., Perlwitz, Ju., Rind, D., Romanou, A., Russell, G.L., Sato, MKi.,
11 Shindell, D.T., Stone, P.H., Sun, S., Tausnev, N., Thresher, D., and Yao, M.S.: Present day
12 atmospheric simulations using GISS ModelE: Comparison to in-situ, satellite and reanalysis
13 data, *J. Climate* 19, 153-192, 2006.
- 14 Schuur, E. A. G., Bockheim, J., Canadell, J. G., Euskirchen, E., Field, C. B., Goryachkin, S. V.,
15 Hagemann, S., Kuhry, P., Lafleur, P. M., Lee, H., Mazhitova, G., Nelson, F. E., Rinke, A., Ro-
16 manovsky, V. E., Shiklomanov, N., Tarnocai, C., Venevsky. S., Vogel, J. G., and Zimov, S. A.:
17 Vulnerability of Permafrost Carbon to Climate Change: Implications for the Global Carbon
18 Cycle, *BioScience*, 58, 701–714, 2008.
- 19 Serreze, M., Walsh, J., Chapin, F., Osterkamp, T., Dyrgerov, M., Romanovsky, V., Oechel, W.,
20 Morison, J., Zhang, T., and Barry, R.: Observational evidence of recent change in the northern
21 highlatitude environment, *Climatic Change*, 46, 159–207, 2000.
- 22 Shiklomanov, N.I., and Nelson, F.E.: Analytic representation of the active layer thickness field,
23 Kuparuk River Basin, Alaska, *Ecological Modeling*, 123(2-3): 105–125. DOI: 10.1016/S0304-
24 3800(99)00127-1, 1999.
- 25 Sitch, S., Smith, B., Prentice, I.C., Arneth, A., Bondeau, A., Cramer, W., Kaplan, J.O., Levis,
26 S., Lucht, W., Sykes, M.T., Thonicke, K., and Venevsky, S.: Evaluation of ecosystem
27 dynamics, plant geography and terrestrial carbon cycling in the LPJ dynamic global vegetation
28 model, *Global Change Biology*, 2003, 9, 2, 2003.
- 29 Slater, A.G., and Lawrence, D.M.: Diagnosing Present and Future Permafrost from Climate
30 Models. *J. Clim.*, 26 (15) 5608-5623, doi: 10.1175/JCLI-D-12-00341.1, 2013.
- 31 Smith, B., Prentice, I. C. and Sykes, M. T.: Representation of vegetation dynamics in the modelling
32 of terrestrial ecosystems: comparing two contrasting approaches within European climate
33 space, *Global Ecology and Biogeography*, 10: 621–637. doi: 10.1046/j.1466-822X.2001.t01-1-
34 00256, 2001.

- 1 Soudzilovskaia, N. A., van Bodegom, P. M., and Cornelissen, J. H.C.: Dominant bryophyte control
2 over high-latitude soil temperature fluctuations predicted by heat transfer traits, field moisture
3 regime and laws of thermal insulation, *Functional Ecology*, 27: 1442–1454. doi: 10.1111/1365-
4 2435.12127S, 2013.
- 5 Stendel M., Romanovsky, V.E., Christensen, J.H., and Sazonova T.: Using dynamical downscaling
6 to close the gap between global change scenarios and local permafrost dynamics, *Global and*
7 *Planetary Change* 56: 203–214. DOI:10.1016/j.gloplacha.2006.07.014, 2007.
- 8 Stevens, B., Giorgetta, M., Esch, M., Mauritsen, T., Crueger, T., Rast, S., Salzmann, M., Schmidt,
9 H., Bader, J., Block, K., Brokopf, R., Fast, I., Kinne, S., Kornblueh, L., Lohmann, U., Pincus,
10 R., Reichler, T., and Roeckner, E.: The atmospheric component of the MPI-M Earth System
11 Model: ECHAM6, *J. Adv. Model. Earth Syst.*, 5, 146–172, doi:10.1002/jame.20015, 2012.
- 12 Taylor, K.E., Stouffer, R.J., and Meehl, G.A.: A summary of the CMIP5 experiment design.
13 PCMDI Tech. Rep., 33 pp. [Available online at [http://cmip-pcmdi.llnl.gov/cmip5/docs/
14 Taylor_CMIP5_design.pdf](http://cmip-pcmdi.llnl.gov/cmip5/docs/Taylor_CMIP5_design.pdf).], 2009.
- 15 Vonder Mühl, D., Hauck, C., and Lehmann, F.: Verification of geophysical models in Alpine
16 permafrost using borehole information, *Annals of Glaciology*, 31, 300-306, 2000.
- 17 Wang, T., Otle, C., Boone, A., Ciais, P., Brun, E., Morin, S., Krinner, G., Piao, S., and Peng, S.:
18 Evaluation of an improved intermediate complexity snow scheme in the ORCHIDEE land
19 surface model, *J. Geophys. Res. Atmos.*, 118, 6064–6079, doi:10.1002/jgrd.50395, 2013.
- 20 Wania R., Ross, I., and Prentice, I.C.: Integrating peatlands and permafrost into a dynamic global
21 vegetation model: 1. Evaluation and sensitivity of physical land surface processes, *GLOBAL*
22 *BIOGEOCHEMICAL CYCLES*, 23, 2009a.
- 23 Wania R., Ross, I., and Prentice, I.C.: Integrating peatlands and permafrost into a dynamic global
24 vegetation model: 2. Evaluation and sensitivity of vegetation and carbon cycle processes,
25 *GLOBAL BIOGEOCHEMICAL CYCLES*, 23, 2009b.
- 26 Wania R., Ross, I., and Prentice, I.C.: Implementation and evaluation of a new methane model
27 within a dynamic global vegetation model : LPJ-WHyMe v1.3.1, *Geoscientific Model*
28 *Development* 3, 565–584, 2010.
- 29 Weedon, G., Gomes, S., Viterbo, P., Österle, H., Adam, J., Bellouin, N., Boucher, O., and Best, M.:
30 The WATCH forcing data 1958-2001: A meteorological forcing dataset for land surface and
31 hydrological models WATCH Tech. Rep. 22, 41 pp., [Available online at [http://www.eu-
32 watch.org/publications/technical-reports](http://www.eu-watch.org/publications/technical-reports).], 2010.
- 33 Westermann, S., Lüers, J., Langer, M., Piel, K., and Boike, J.: The annual surface energy budget of
34 a high-arctic permafrost site on Svalbard, Norway, *The Cryosphere*, 3, pp. 245-263,
35 doi:10.5194/tc-3-245-2009, 2009.

- 1 Westermann, S., Wollschläger, U., and Boike, J.: Monitoring of active layer dynamics at a
2 permafrost site on Svalbard using multi-channel ground-penetrating radar, *The Cryosphere*, 4,
3 pp. 475-487, doi: 10.5194/tc-4-475-2010, 2010.
- 4 Westermann, S., Langer, M., and Boike, J.: Spatial and temporal variations of summer surface
5 temperatures of high-arctic tundra on Svalbard - Implications for MODIS LST based permafrost
6 monitoring, *Remote Sensing of Environment*, 115 (3), 908 – 922,
7 doi:10.1016/j.rse.2010.11.018, 2011.
- 8 Wolf, A., Callaghan, T., and Larson, K.: Future changes in vegetation and ecosystem function of
9 the Barents Region, *Clim. Change*, 87, 51–73, 2008.
- 10 ZackenbergGIS, <http://dmugisweb.dmu.dk/zackenberggis/datapage.aspx>, last access: 10 September
11 2012.
- 12 Zhang, T.: Influence of the seasonal snow cover on the ground thermal regime: An overview, *Rev.*
13 *Geophys.*, 43, RG4002, doi:10.1029/2004RG000157, 2005.
- 14 Zhang, W., Miller, P.A., Smith, B., Wania, R., Koenigk, T. and Döscher, R.: Tundra shrubification
15 and tree-line advance amplify arctic climate warming: results from an individual-based dynamic
16 vegetation model, *Environmental Research Letters* 8: 034023, 2013.

17
18
19
20
21
22
23
24
25
26
27
28
29
30
31
32
33
34
35
36
37
38
39

1 Table 1: Model details related to soil heat transfer

	JSBACH	ORCHIDEE	JULES	COUP	HYBDRID8	LPJ-GUESS
Soil freezing	Yes	Yes	Yes	Yes	Yes	Yes
Soil heat transfer method	Conduction	Conduction	Conduction Advection	Conduction Advection	Conduction Advection	Conduction
Dynamic soil heat transfer parameters	Yes	Yes	Yes	Yes	Yes	Yes
Soil depth	10m	43m	3m	Variable (>5m)	Variable (>5m)	2m
Bottom boundary condition	Zero heat flux	Geothermal heat flux (0.057 W/m ²)	Zero heat flux	Geothermal heat flux (0.011 W/m ²)	Zero heat flux	Zero heat flux
Snow layering	5 layers	3 layers	3 layers	1 layer	No snow representation	1 layer
Dynamic snow heat transfer parameters	No	Yes	Yes	Yes	-	Yes (only heat capacity)
Insulating vegetation cover	10cm moss layer	-	-	-	-	Site-specific litter layer
Model timestep	30min	30min	30min	30min	30min	1day

2
3
4
5
6
7
8
9
10
11
12
13
14
15
16
17
18
19
20
21

1 Table 2: Site details

	NUUK	SCHILTHORN	SAMOYLOV	BAYELVA
Latitude	64.13° N	46.56° N	72.4° N	78.91° N
Longitude	51.37° W	7.08° E	126.5° E	11.95° E
Mean annual air temperature	-1.3 °C	-2.7 °C	-13 °C	-4.4 °C
Mean annual ground temperature	3.2 °C	-0.45 °C	-10 °C (?)	-2/-3 °C
Annual precipitation	900 mm	1963 mm	200 mm	400 mm
Avg. length of snow cover	7 months	9.5 months	9 months	9 months
Vegetation cover	Tundra	Barren	Tundra	Tundra

2
3
4
5
6
7
8
9
10
11
12
13
14
15
16
17
18
19
20
21
22
23
24
25
26
27
28
29

1 Table 3: Details of driving data preparation for site simulations

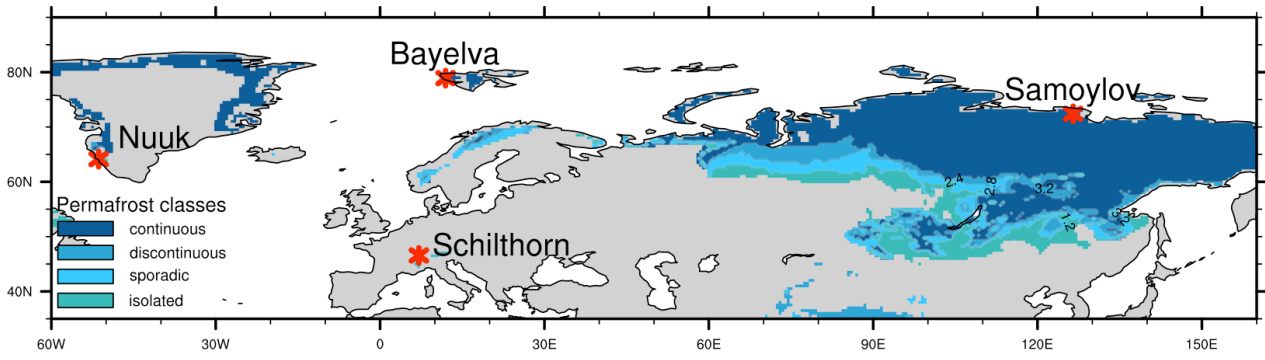
	NUUK	SCHILTHORN	SAMOYLOV	BAYELVA	
ATMOSPHERIC FORCING VARIABLES	Air temperature	<i>In-situ</i>	<i>In-situ</i>	<i>In-situ</i>	
	Precipitation	<i>In-situ</i>	<i>In-situ</i>	<i>In-situ</i> (snow season from WATCH)	
	Air pressure	<i>In-situ</i>	WATCH	WATCH	
	Atm. humidity	<i>In-situ</i>	<i>In-situ</i>	<i>In-situ</i>	
	Incoming longwave radiation	<i>In-situ</i>	<i>In-situ</i>	<i>In-situ</i>	
	Incoming shortwave radiation	<i>In-situ</i>	<i>In-situ</i>	WATCH	
	Net radiation	<i>In-situ</i>	-	<i>In-situ</i>	
	Wind speed	<i>In-situ</i>	<i>In-situ</i>	<i>In-situ</i>	
	Wind direction	<i>In-situ</i>	-	<i>In-situ</i>	
	Time period	26.06.2008-31.12.2011	01.10.1999-30.09.2008	14.07.2003-11.10.2005	01.01.1998-31.12.2009
STATIC SOIL PARAMETERS	Soil porosity	46%	50%	60%	
	Soil field capacity	36%	44%	31%	
	Mineral soil depth	36cm	710cm	800cm	
	Dry soil heat capacity	2.213x10 ⁶ (Jm ⁻³ K ⁻¹)	2.203x10 ⁶ (Jm ⁻³ K ⁻¹)	2.1x10 ⁶ (Jm ⁻³ K ⁻¹)	2.165x10 ⁶ (Jm ⁻³ K ⁻¹)
	Dry soil heat conductivity	6.84 (Wm ⁻¹ K ⁻¹)	7.06 (Wm ⁻¹ K ⁻¹)	5.77 (Wm ⁻¹ K ⁻¹)	7.93 (Wm ⁻¹ K ⁻¹)
	Sat. hydraulic conductivity	2.42 x10 ⁻⁶ (ms ⁻¹)	4.19 x10 ⁻⁶ (ms ⁻¹)	2.84 x10 ⁻⁶ (ms ⁻¹)	7.11 x10 ⁻⁶ (ms ⁻¹)
	Saturated moisture potential	0.00519 (m)	0.2703 (m)	0.28 (m)	0.1318 (m)

2
3
4
5
6
7
8
9
10
11
12
13
14
15

1 Table 4: Details of model spin up procedures

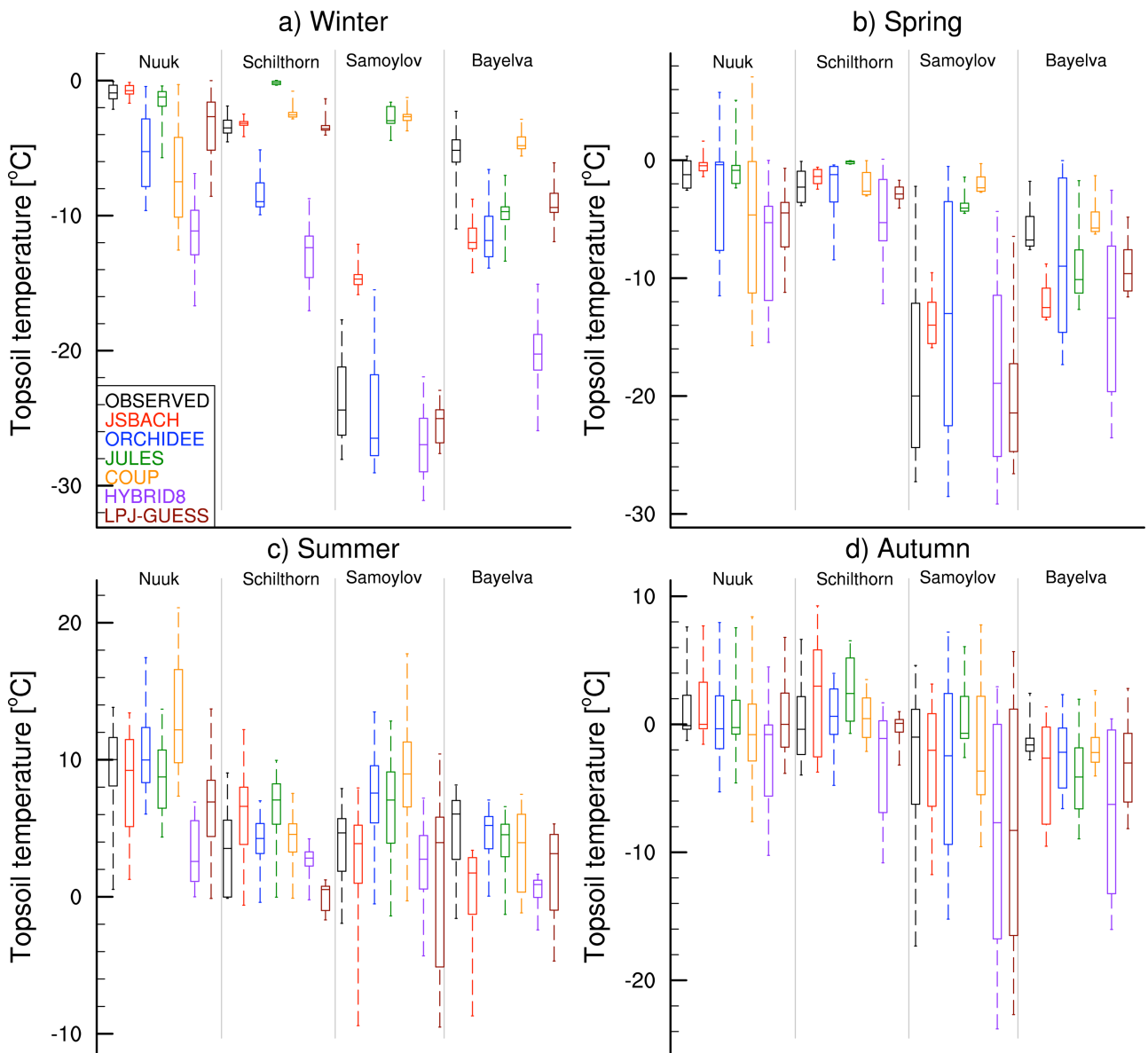
	JSBACH	ORCHIDEE	JULES	COUP	HYBRID8	LPJ-GUESS
Spin-up data	Observed climate	Observed climate	Observed climate	Observed climate	Observed climate	WATCH* data
Spin-up duration	50 years	10,000 years	50 years	10 years	50 years	500 years

2 *500 years forced with monthly WATCH reanalysis data from the 1901-1930 period, followed by daily
 3 WATCH forcing from 1901-until YYYY-MM-DD, then daily site-data.
 4
 5
 6
 7
 8
 9
 10
 11
 12
 13
 14
 15
 16
 17
 18
 19
 20
 21
 22
 23
 24
 25
 26
 27
 28
 29
 30
 31



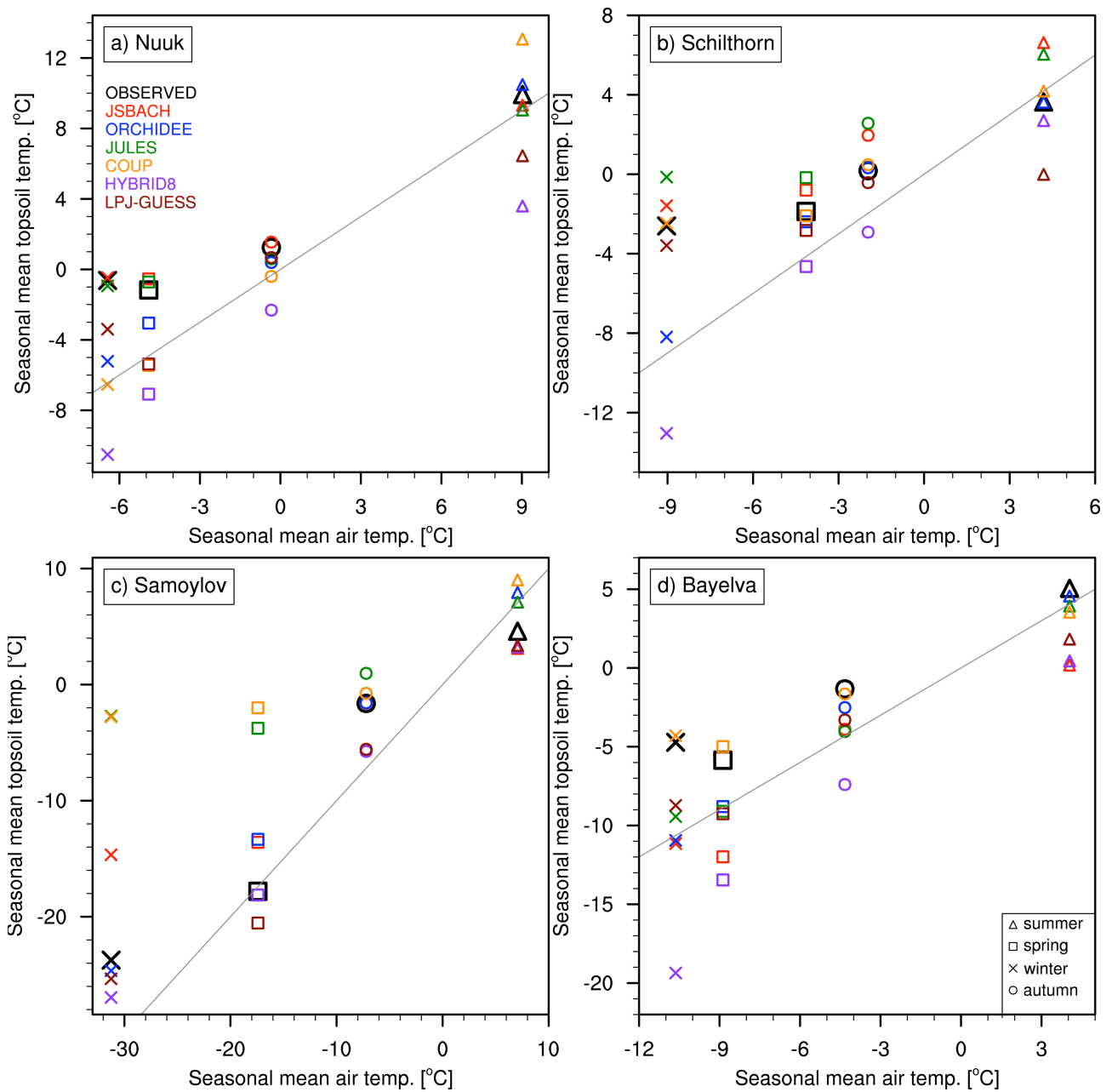
1
2
3
4
5
6
7
8
9
10

Figure 1: Site location map.



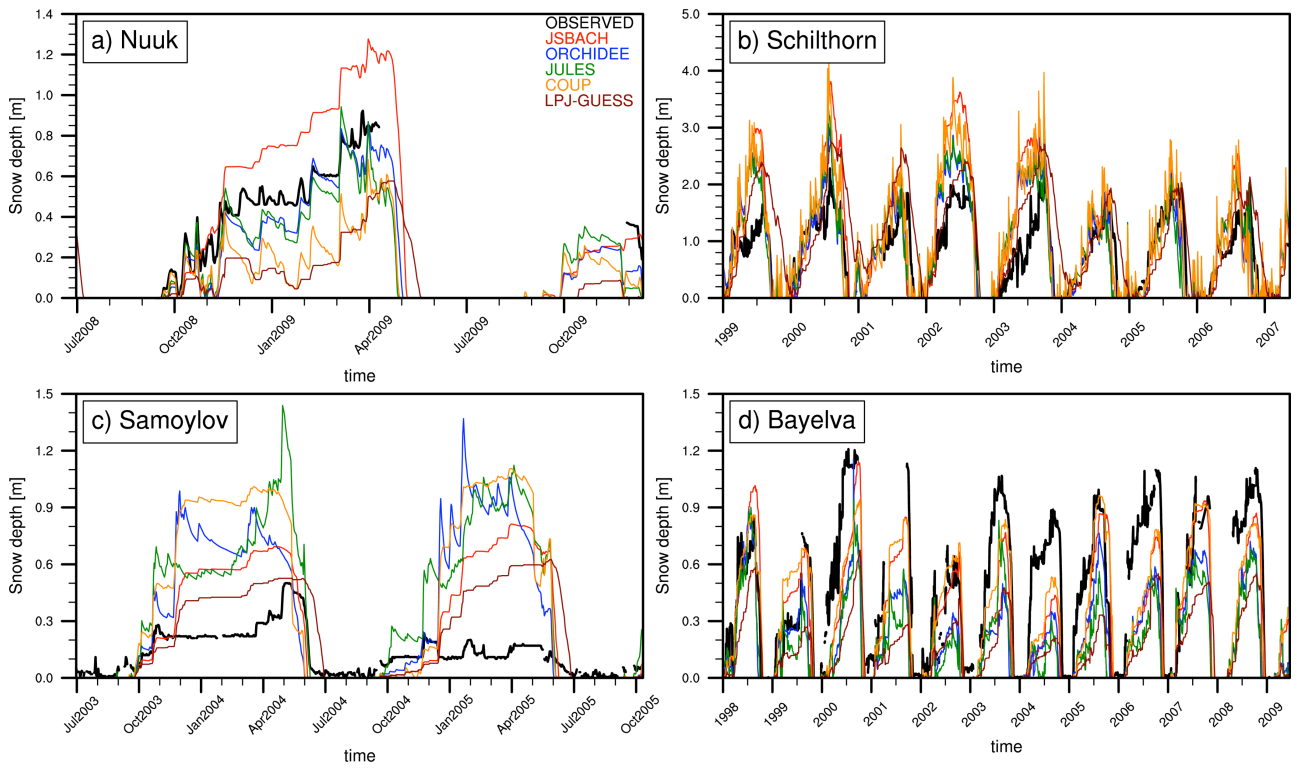
1
2
3
4
5
6
7
8

Figure 2: Box plots showing the topsoil temperature for observation and models for different seasons. Boxes are drawn with 25th percentile, mean and 75th percentiles while the whiskers show the min and max values. Seasonal averages of soil temperatures are used for calculating seasonal values. Each plot includes 4 study sites divided by the gray lines. Black boxes show observed values and colored boxes distinguish models. See Table A1 in Appendix-A for exact soil depths used in this plot.



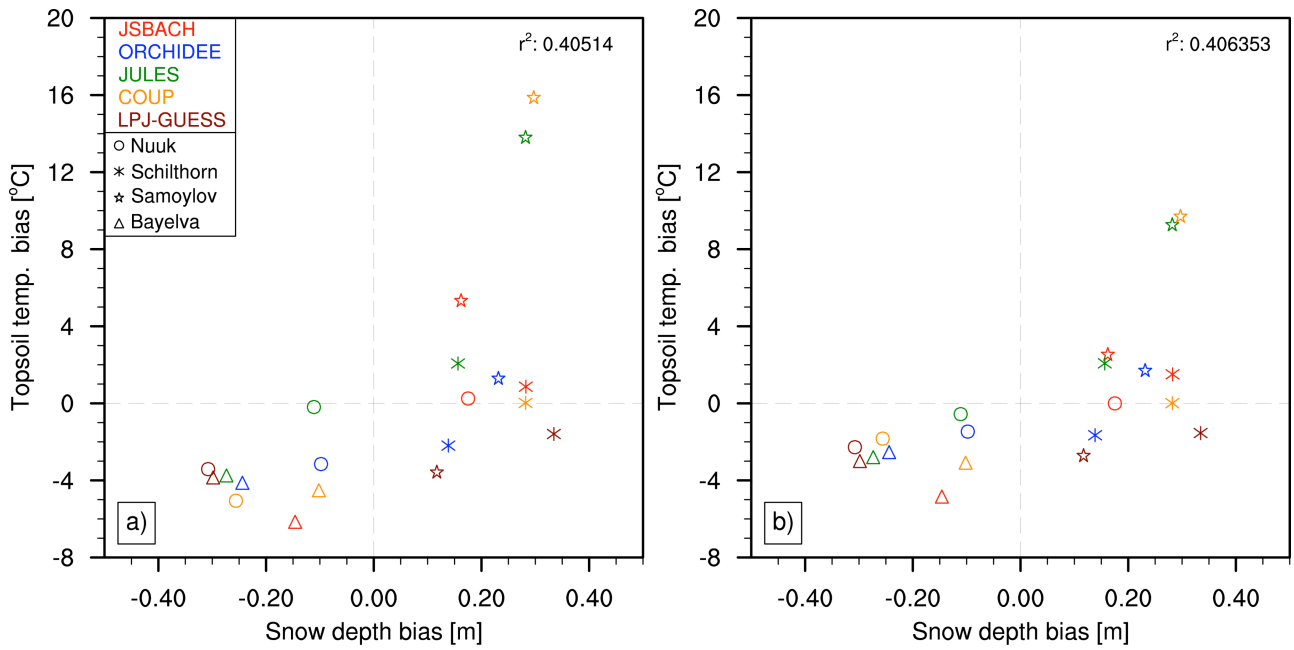
1
2

3 Figure 3: Scatter plots showing air/topsoil temperature relation from observations and models at each site for different
 4 seasons. Seasonal mean observed air temperature is plotted against the seasonal mean modeled topsoil temperature
 5 separately for each site. Black markers are observed values, colors distinguish models and markers distinguish seasons.
 6 Gray lines represent the 1:1 line. See Table A1 in Appendix-A for exact soil depths used in this plot.



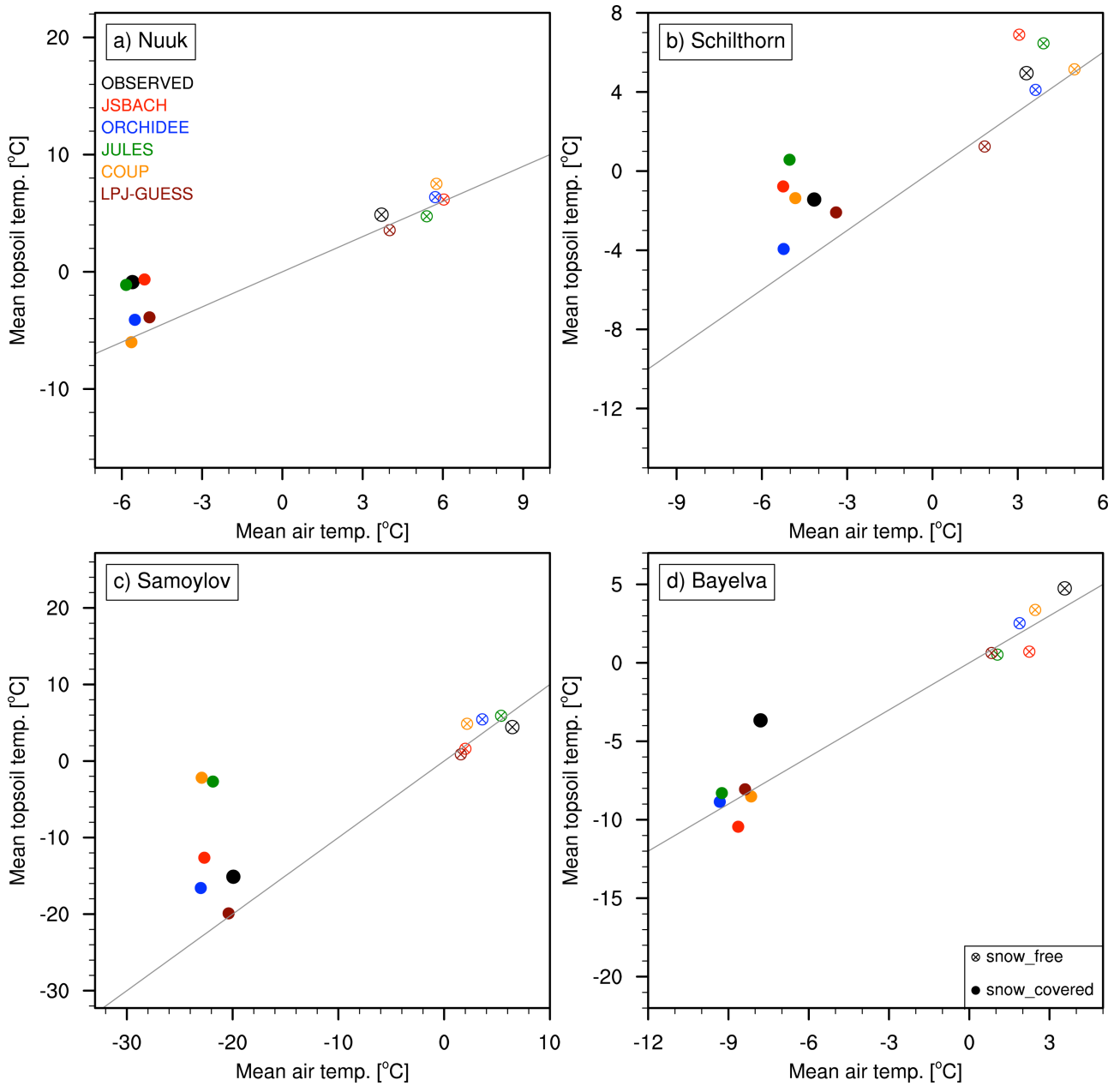
1
2
3
4
5
6
7
8
9
10
11
12
13
14

Figure 4: Time series plots of observed and simulated snow depths for each site. Thick black lines are observed values and colored lines distinguish simulated snow depths from models.



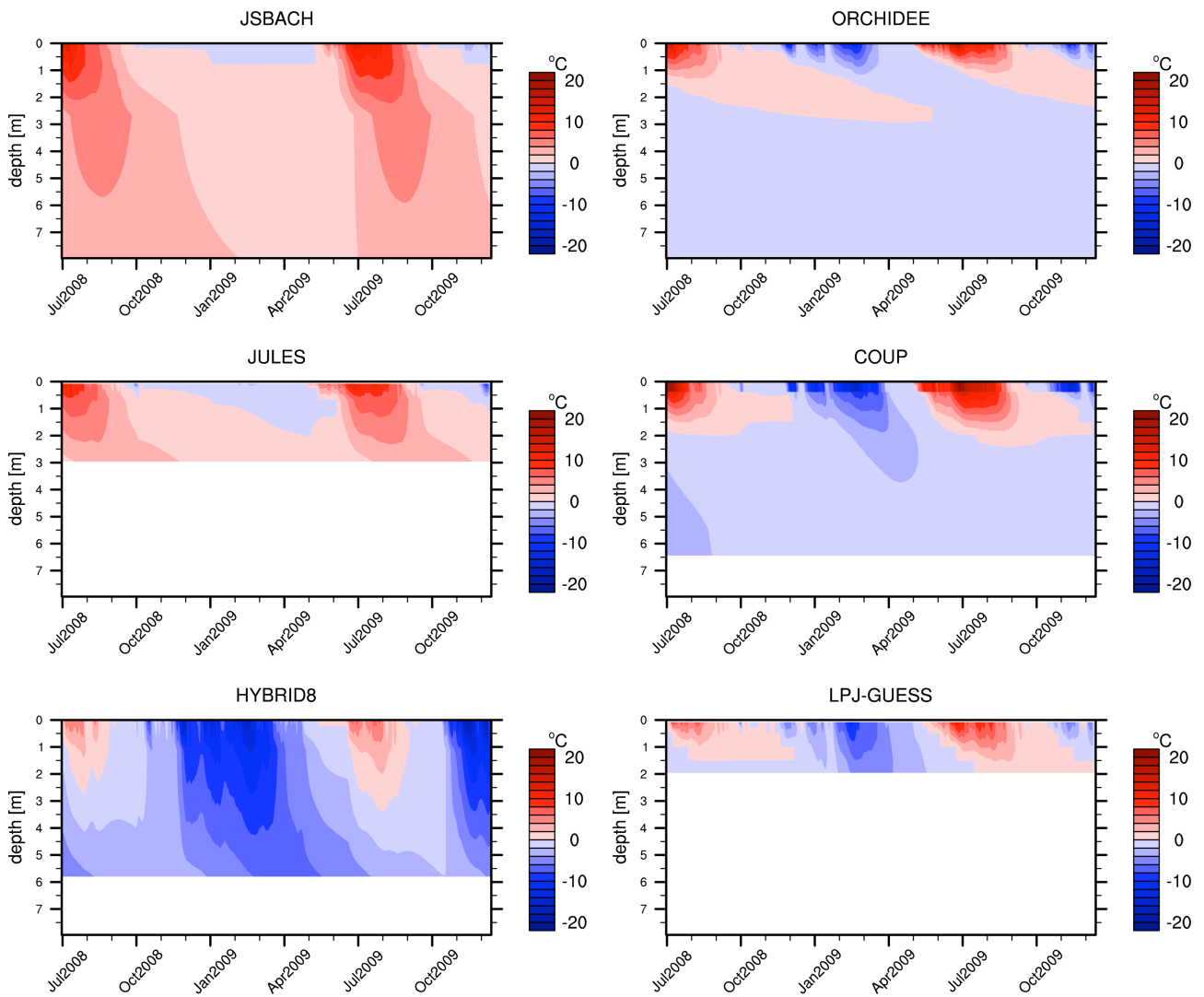
1
2
3
4
5
6
7
8
9

Figure 5: Scatter plots showing the relation between snow depth bias and topsoil temperature bias during snow season (a) and the whole year (b). Snow season is defined separately for each model, by taking snow depth values over 5 cm to represent the snow-covered period. The average temperature bias of all snow covered days is used in (a), and the temperature bias in all days (snow covered and snow free seasons) is used in plot (b). Markers distinguish sites and colors distinguish models. See Table A1 in Appendix-A for exact soil depths used in this plot.



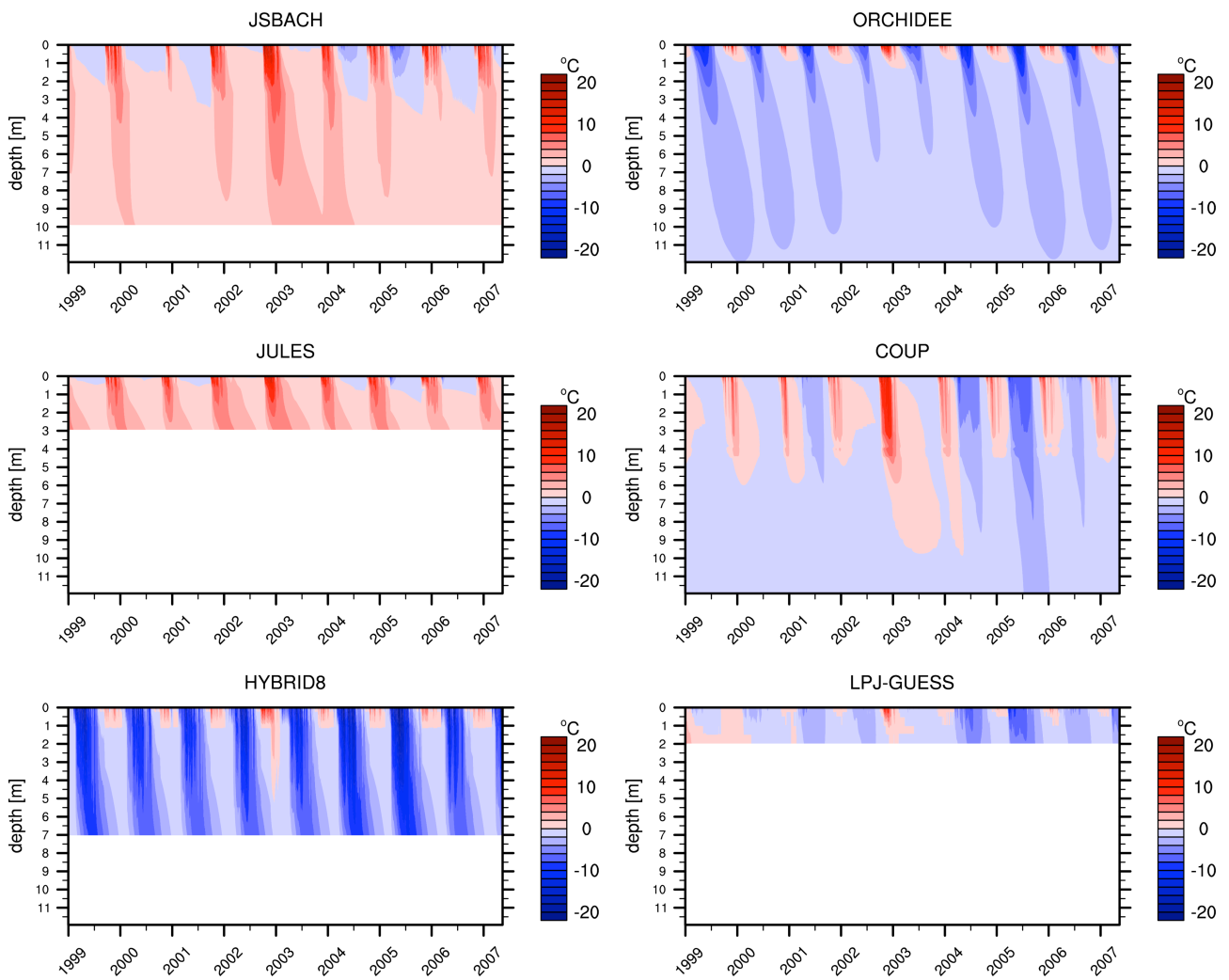
1
2
3
4
5
6
7
8
9
10

Figure 6: Scatter plots showing air/topsoil temperature relation from observations and models at each site for snow and snow-free seasons. Snow season is defined separately for observations and each model, by taking snow depth values over 5 cm to represent the snow-covered period. The average temperature of all snow covered (or snow free) days of the simulation period is used in the plots. Markers distinguish snow and snow free seasons and colors distinguish models. Gray lines represent the 1:1 line. See Table A1 in Appendix-A for exact soil depths used in this plot.



1
2
3
4
5

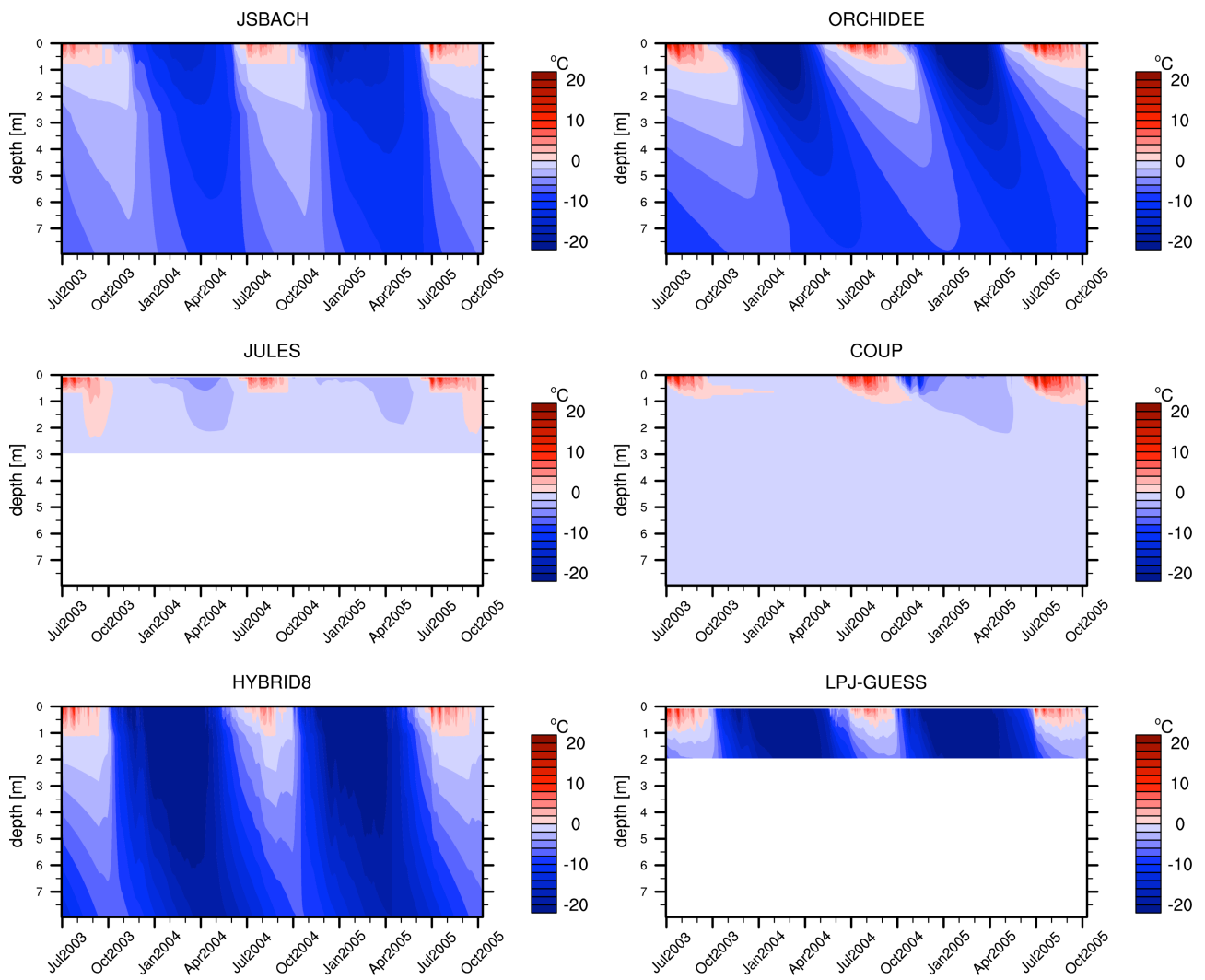
Figure 7: Time-depth plot of soil temperature evolution at the Nuuk site for each model. Simulated soil temperatures are interpolated into 200 evenly spaced nodes to represent a continuous vertical temperature profile. The deepest soil temperature calculation is taken as the bottom limit for each model (no extrapolation applied).



1

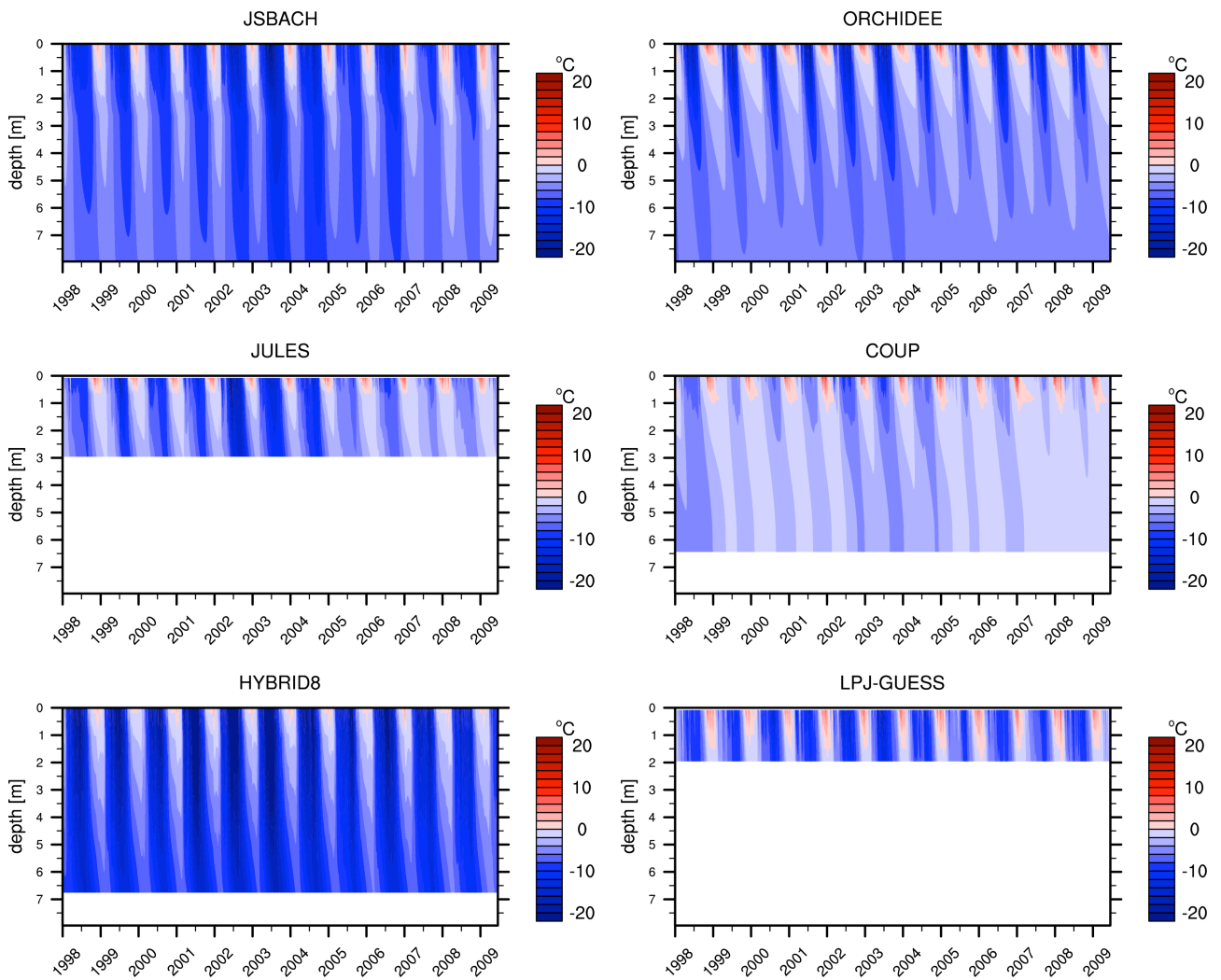
2

3 Figure 8: Time-depth plot of soil temperature evolution at Schilthorn site for each model. Simulated soil temperatures
 4 are interpolated into 200 evenly spaced nodes to represent a continuous vertical temperature profile. The deepest soil
 5 temperature calculation is taken as the bottom limit for each model (no extrapolation applied).



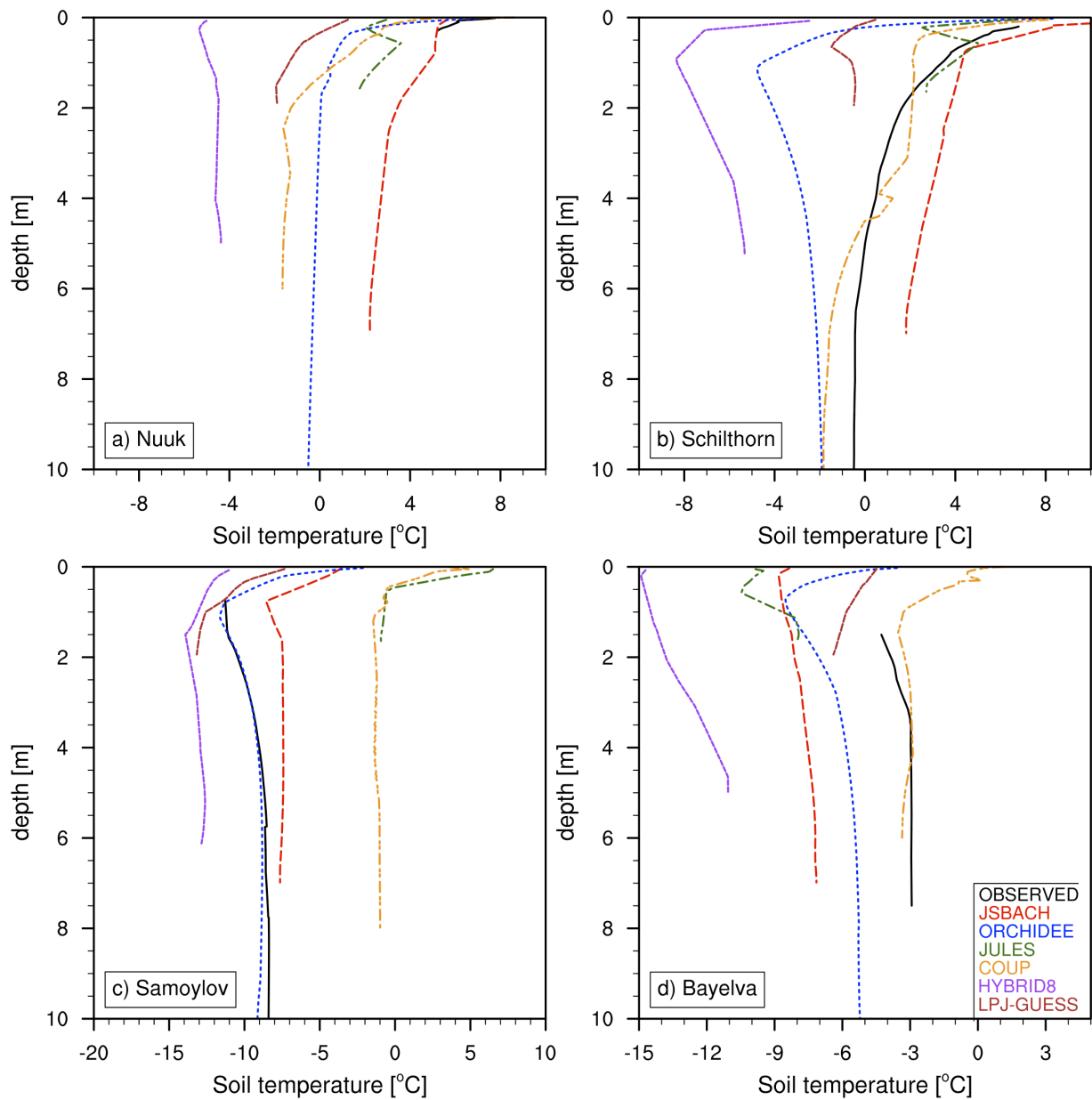
1
2

3 Figure 9: Time-depth plot of soil temperature evolution at Samoylov site for each model. Simulated soil temperatures
4 are interpolated into 200 evenly spaced nodes to represent a continuous vertical temperature profile. The deepest soil
5 temperature calculation is taken as the bottom limit for each model (no extrapolation applied).

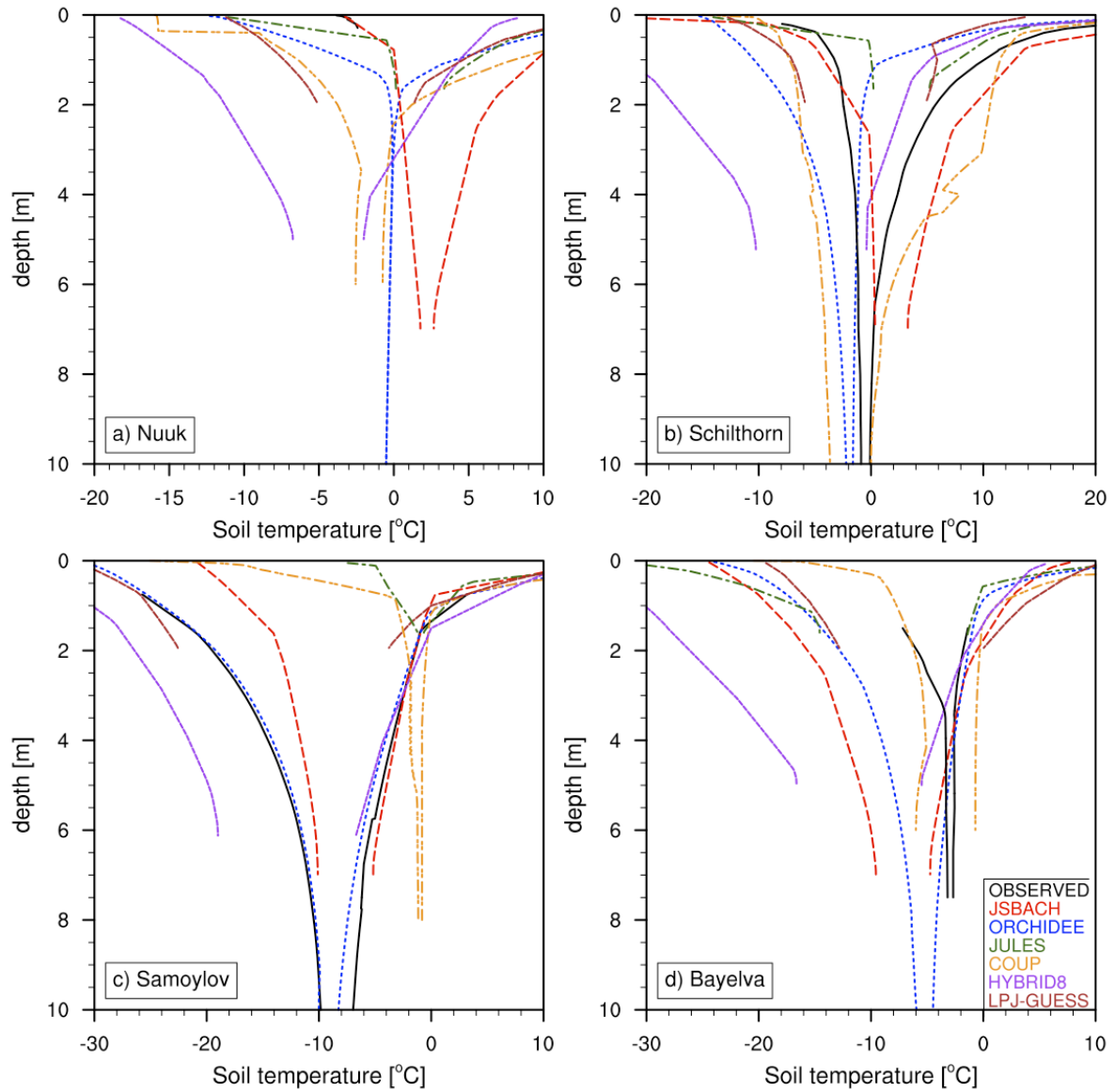


1
2

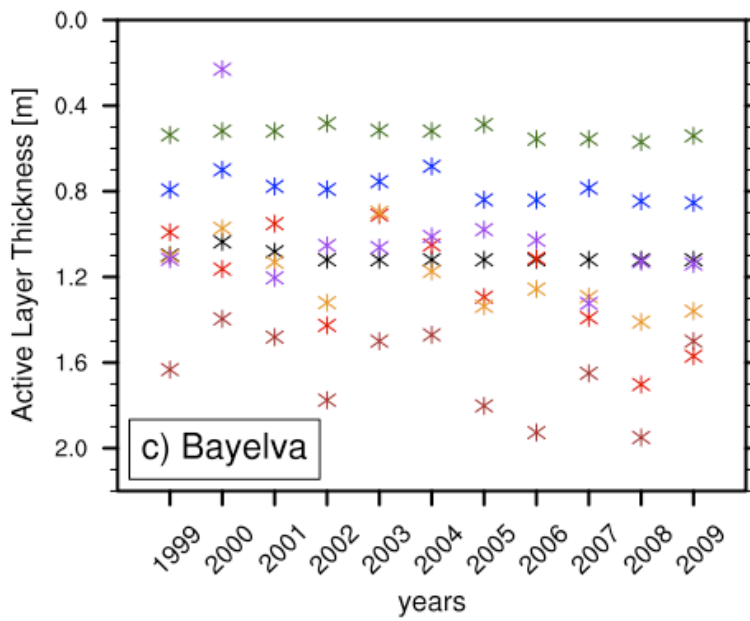
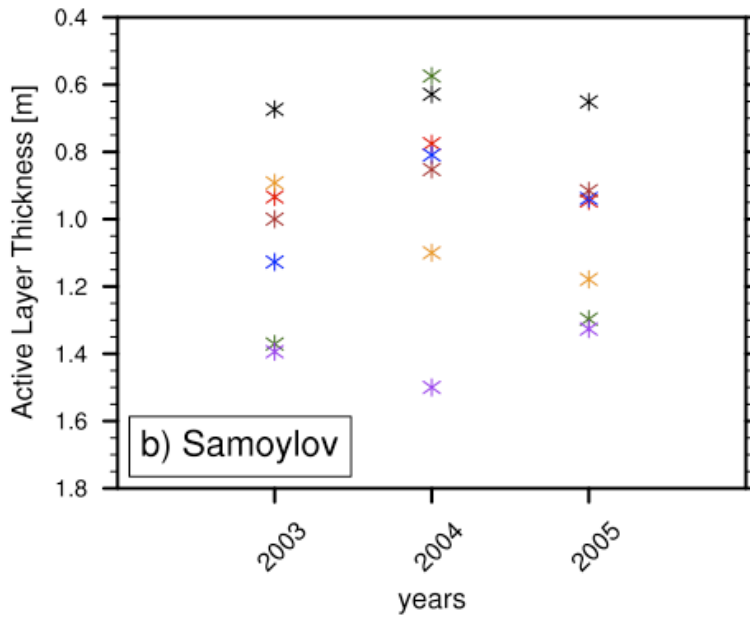
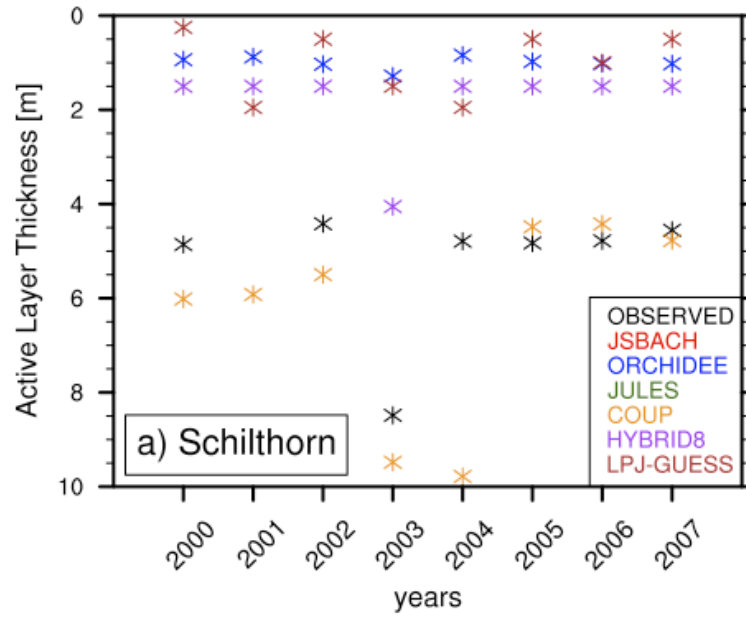
3 Figure 10: Time-depth plot of soil temperature evolution at Bayelva site for each model. Simulated soil temperatures
4 are interpolated into 200 evenly spaced nodes to represent a continuous vertical temperature profile. The deepest soil
5 temperature calculation is taken as the bottom limit for each model (no extrapolation applied).



1
 2 Figure 11: Vertical profiles of annual soil temperature means of observed and modeled values at each site. Black thick
 3 lines are the observed values and colored dashed lines distinguish models. (Samoylov and Bayelva observations are
 4 from borehole data).



1
2 Figure 12: Soil temperature envelopes showing the vertical profiles of soil temperature amplitudes of each model at
3 each site. Soil temperature values of observations (except Nuuk) and each model are interpolated to finer vertical
4 resolution and max and min values are calculated for each depth to construct max and min curves. For each color, the
5 right line is the maximum and the left line is the minimum temperature curve. Black thick lines are the observed values
6 and colored dashed lines distinguish models.



1 Figure 13: Active layer thickness (ALT) values for each model and observation at the three permafrost sites. ALT
2 calculation is performed separately for models and observations by interpolating the soil temperature profile into finer
3 resolution and estimating the maximum depth of 0°C for each year. Plots a, b and c show the temporal change of ALT
4 at Schilthorn (2001 is omitted because observations have major gaps, also JSBACH and JULES are excluded as they
5 simulate no permafrost at this site), Samoylov and Bayelva respectively, while the lower-right plot shows their relation
6 to mean annual air temperature (MAAT). Colors distinguish models/observations and markers distinguish sites.